



Calhoun: The NPS Institutional Archive
DSpace Repository

Theses and Dissertations

1. Thesis and Dissertation Collection, all items

1951

Applications of inertial navigation to underwater warfare

Cook, Robert H.; Gustafson, Boyd E.

Massachusetts Institute of Technology

<https://hdl.handle.net/10945/13946>

Downloaded from NPS Archive: Calhoun



Calhoun is the Naval Postgraduate School's public access digital repository for research materials and institutional publications created by the NPS community. Calhoun is named for Professor of Mathematics Guy K. Calhoun, NPS's first appointed -- and published -- scholarly author.

Dudley Knox Library / Naval Postgraduate School
411 Dyer Road / 1 University Circle
Monterey, California USA 93943

<http://www.nps.edu/library>

APPLICATIONS OF INERTIAL NAVIGATION TO
UNDERWATER WARFARE

ROBERT H. COOK
BOYD E. GUSTAFSON

LIBRARY
U.S. NAVAL POSTGRADUATE SCHOOL
MONTEREY, CALIFORNIA

This document has been approved for public
release and sale; its distribution is unlimited.

#; Meunster 1/2/69

APPLICATIONS OF INERTIAL NAVIGATION
TO UNDERWATER WARFARE

by

ROBERT H. COOK, Lieutenant, U. S. N.
B.S., U.S. Naval Academy, 1943
B.S., U.S. Naval Post Graduate School, 1950

BOYD E. GUSTAFSON, Lieutenant, U. S. N.
B.S., U.S. Naval Academy, 1943
B.S., U.S. Naval Post Graduate School, 1950

SUBMITTED IN PARTIAL FULFILLMENT OF THE
REQUIREMENTS FOR THE DEGREE OF
MASTER OF SCIENCE
IN MECHANICAL ENGINEERING

at

MASSACHUSETTS INSTITUTE OF TECHNOLOGY
1951

~~CONFIDENTIAL~~
Thesis

C7475

This document contains information affecting the national defense of the United States within the meaning of the Espionage Act, 50 U.S.C., 31 and 32, as amended. Its transmission or the revelation of its contents in any manner to an unauthorized person is prohibited by law.

APPLICATIONS OF INERTIAL NAVIGATION
TO UNDERWATER WARFARE

by

Robert H. Cook
and
Boyd E. Gustafson

Submitted for the degree of Master of Science in the Department of Mechanical Engineering at Massachusetts Institute of Technology on May 18, 1951.

ABSTRACT

The true submersible, capable of extended operating periods without surfacing, has long been desired. Present day submarines must surface in order to charge batteries. Celestial navigation, therefore, is available as a by-product of normal operating procedures. With the advent of the submarine capable of extended periods of operation submerged, it will be necessary to provide a method of navigation that will not require the submarine to surface, if full advantage is to be taken of her other characteristics.

The Instrumentation Laboratory, Massachusetts Institute of Technology, proposes, as a solution to the navigation problem, the application of inertial techniques employing gyros to provide the inertial reference and stabilized platforms to provide position indication. The problem is thus one of measuring the change in a direction, that of the true vertical, with respect to inertial space.

Inertial techniques are being applied to air navigation. For these applications, it is assumed that the carrying vehicle departs from a stable base, where a well defined vertical and azimuth direction are available for "lining-up" the system prior to departure. A somewhat different problem exists for a submarine underway at sea. Here, there are no well

20400

established references available; hence, the boundary conditions are largely unknown.

A study of possible systems for applying inertial methods to submarine navigation is currently underway at the Instrumentation Laboratory, Massachusetts Institute of Technology. A report⁽¹⁵⁾ has been issued on the initial phase of the study, in which only undamped systems employing ideal components were considered. A self-settling system, however, must employ damping, which, together with component performance, will affect the accuracy of the system; hence, the complete study will consider these effects on system performance. Furthermore, the resulting system must have a period approaching the 84.4-minute Schuler-tuning condition if it is to be effective. This fact implies that the transient effects due to disturbances imposed upon the system will have a duration measured in terms of hours. It would therefore be desirable to have some means available for predicting the errors resulting from such disturbances.

This thesis suggests that the mean-square error in position can be predicted for any particular time during the duration of the transient by using the power spectral density of the disturbance and a function defined as the transient transfer function, and that this method may be applied in the design stage to arrive at component performance specifications.

For illustration, the equations for one proposed inertial system, using nonideal components which in themselves generate uncertainties or disturbances, have been derived and the application of the proposed method for evaluating the resulting errors is shown.

It is regretted that lack of time and non-availability of equipment prevented a more thorough study of the problem. However, from the work completed, it appears unsafe to design a system on the basis of steady-state servoanalysis techniques where the solution of the problem during the duration of the transient is also of primary importance. This conclusion is based upon the fact that the response of the third-order system studied to a forcing input $e^{j\omega t}$ made an initial excursion which was up to several times as large as the steady-state response. Furthermore, the ratio of the initial excursion to the steady-state response increased with an increasing frequency, whereas the time at which the maximum excursion occurred did not appear to be any well behaved function of the frequency.

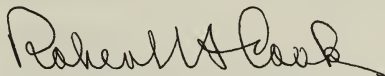
~~CONFIDENTIAL~~
UNCLASSIFIED

May 18, 1951

Prof. Joseph S. Newell
Secretary of the Faculty
Massachusetts Institute of Technology
Cambridge 39, Massachusetts

Dear Professor Newell:

In accordance with the regulations of the faculty, we hereby submit a thesis entitled APPLICATIONS OF INERTIAL NAVIGATION TO UNDERWATER WARFARE, in partial fulfillment of the requirements for the degree of Master of Science in Mechanical Engineering.



Boyd E Gustafson

~~CONFIDENTIAL~~
UNCLASSIFIED

ACKNOWLEDGMENT

The authors express their appreciation to those personnel of the Instrumentation Laboratory, Massachusetts Institute of Technology, who assisted in the preparation of this thesis. In particular, we wish to thank Dr. W. Wrigley and Dr. J. H. Laning Jr. for their interest and assistance in the progress of this thesis; Mr. Forrest E. Houston and Mr. John Hovorka for their guidance in the theoretical aspects of the problem; and the personnel of Jackson & Moreland for their aid in the preparation of the printed form of the thesis.

The graduate work, for which this thesis is a partial requirement, was performed while the authors were assigned to Naval Training School, Massachusetts Institute of Technology. This thesis was prepared under the auspices of DIC Project 6796, sponsored by the Office of Naval Research under contract N5ori-07850.

TABLE OF CONTENTS

	<u>Page</u>
ABSTRACT	iii
CHAPTER 1 DISCUSSION OF INERTIAL NAVIGATION	1
Introduction	1
Inertial Navigation	1
CHAPTER 2 PROPOSED METHOD FOR ARRIVING AT COMPONENT SPECIFICATIONS	12
Uncertainties in Components	12
The Transient Transfer Function	16
The Weighting Function	19
CHAPTER 3 ANALYSIS OF VERTICAL INDICATORS	21
General	21
Undamped Vertical Indicator	21
Damped Vertical Indicator	25
APPENDIX A VERTICAL INDICATION	50
APPENDIX B POSITION INDICATION BY OPEN-CHAIN INTEGRATION OF THE INDICATED VER- TICAL	70
APPENDIX C OPTIMIZATION OF SYSTEM PARAMETERS	75
APPENDIX D METHOD USED IN THE DETERMINATION OF SYSTEM PERFORMANCE CHARACTERISTICS	86
REFERENCES	91

OBJECT

To investigate the possible application of a self-contained inertial system to the navigation of submerged vehicles.

CHAPTER 1

DISCUSSION OF INERTIAL NAVIGATION

INTRODUCTION

The problem of navigation of a submerged vehicle is of interest in view of proposed submarine operating characteristics that enable extended submerged periods. These characteristics will make it necessary to navigate from the submerged vehicle for considerable periods of time, with some degree of accuracy, and without reference to external information. Solution of the problem of long-range all-weather aircraft navigation has been attempted by inertial techniques. An attempt to apply similar techniques to the navigation of underwater vehicles is only now being investigated. ⁽¹⁵⁾

Six systems for inertial navigation have been proposed and studied in the undamped form, using ideal components. ⁽¹⁵⁾ This thesis proposes to investigate the effects on the performance of one of these systems when nonideal components, which introduce uncertainties such as gyro drift, integrator drift, etc., are included in the system, and further, to extend the study to the damped system.

INERTIAL NAVIGATION

Navigation is the science of guidance of a vehicle over the Earth, over or through its waters, and through its atmosphere. This guidance involves a two-fold function of indication and control. Indication is the comparison of the indicated position of the vehicle with some reference fixed in the Earth. This comparison may be used to obtain the distance to a destination and the direction the vehicle must move to reach that destination. It has thus effectively produced the control signal.

Piloting, which is the simplest form of guidance, is ignored in this discussion, because it is assumed that no optical line of sight is available. The substitution of electro-magnetic beams for optical lines of sight, and the substitution of time intervals for distance information, leave the essentials of piloting in the guidance problem. This guidance system is subject to interference, either natural or man made. The desire to minimize interference has stimulated the search for a self-contained guidance system operating on such natural earth phenomena as are effectively interference proof.

Inertial navigation can be regarded as a precision dead-reckoning method in which measurements are made with respect to inertial space rather than with respect to the water surrounding the vehicle. Conventional celestial navigation is a form of partial navigation in which stars represent the inertial space references; but the requirement for submerged operation precludes the consideration of celestial systems. Full inertial systems use gyroscopes for inertial reference.

Physical Factors Available for Guidance

The natural phenomena associated with the Earth that offer possibilities for use with a self-contained guidance system include data from the medium surrounding its vehicle, the Earth's electric field, the Earth's magnetic field, and the Earth's gravity field. References (13) and (1) discuss each of these possibilities in general and conclude that the Earth's gravity field appears to be the best-suited source of data for a self-contained guidance system.

The mass of the Earth has associated with it a gravitational field, which field is essentially radial to the center of the Earth and has no poles. The direction of this gravitational field could be readily determined by a plumb bob if the Earth were non-rotating. Due to a basic law of physics, namely, the principle of equivalence in the general theory of relativity, that gravitational mass is equivalent to inertial mass, the daily rotation of the Earth produces a centrifugal acceleration that also affects the plumb bob. The vector resultant of the Earth's gravitational field and the centrifugal force field is defined as the Earth's gravity field, and the direction of this essentially radial gravity field is unique at any given point on the Earth (Fig. 1-1).

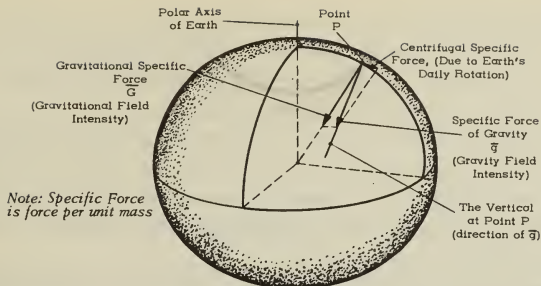


Fig. 1-1 Gravitational field intensity and gravity field intensity (the vertical).

The Earth itself is subject to the equivalence of gravitational and inertial effects. The associated centrifugal force field causes the Earth to bulge at the equator, giving it a nearly ellipsoidal or spheroidal shape. The figure that a fluid body with the mass distribution and daily rotation of the Earth would have is defined as the geoid. Attempts are made to represent the geoid by an associated reference ellipsoid for the basis of geodetic measurements and map data. The surface of the geoid is represented by mean sea level, which is everywhere an equipotential surface of the Earth's gravity field. Because the geoid does not have a consistently smooth surface, the vertical is not in general parallel to the normal to the reference ellipsoid at the same position. The angle between the vertical and the ellipsoid normal is called the deflection of the vertical. This deflection is generally less than 0.30 milliradian ; and generally, the largest marine deflections occur in regions of rapid changes in ocean depth.

In general, variations in the deflection of the vertical can be considered to be quasi-static at submarine speeds, and can be expected to have no dynamic effect on the operation of submarine inertial navigation systems.

Basic Principles of Inertial Navigation

The vertical, which is the direction of the specific force of gravity, is unique at any point on the Earth and is the basis of the astronomical position of that point. Astronomical position is a direction relative to the

Earth and has two components:

1. Astronomical latitude, the angle between the equatorial plane and the vertical at the located point. This quantity is unique because the Earth's polar axis has a unique spatial direction.

2. Astronomical longitude, the angle between the plane through the Earth's polar axis containing an arbitrary vertical (e. g. , that at Greenwich) and the plane through the polar axis containing the located vertical. This quantity itself is not unique because of its arbitrary reference, but difference of longitude is unique.

Astronomical position data will not agree, in general, with geodetic position data (on which maps are based) due to the before mentioned deflection of the vertical. However, position data determined by vertical indication and corresponding map data should agree in the case of small land masses whose positions have been plotted from astronomical data.

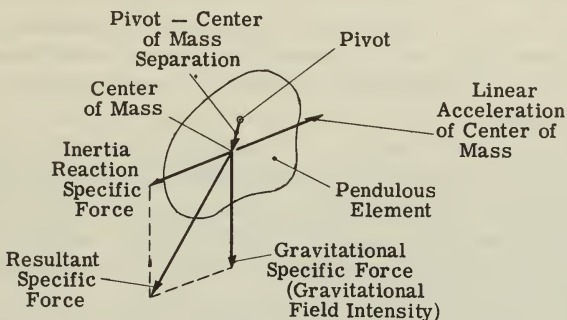
The fundamental problem associated with inertial navigation is then the indication of the vertical inside a self-contained vehicle that is undergoing additional linear accelerations. It is this problem which has been considered in detail in Reference (15).

Theory of Vertical Indicators

The simplest vertical indicator is the plumb bob or pendulum. A pendulous element is defined as a system free to rotate about a point, so that it assumes a preferred orientation under the influence of impressed external forces. If the suspension-point is not accelerated with respect to the Earth, the pendulous element can provide a precise indication of the true vertical, i. e. , the direction of gravity. If the suspension-point is accelerated with respect to the Earth, the pendulous element tends to indicate the apparent vertical, i. e. , the direction of the resultant specific force.

When the pivot of the pendulous element is accelerated, a reaction torque acts on the center of the mass of the element, producing a torque which causes the element to lag behind the pivot. To study the effects of an acceleration without introducing the effects of the mass of the element, it is convenient to discuss the motion in terms of force per unit mass, i. e. , in terms of the inertia reaction specific force associated with the acceleration. An inertia reaction specific force has the magnitude of its associated acceleration (though expressed in different units) and is opposite in direc-

tion. Figure 1-2 is a force diagram for an accelerated pendulous element in a gravitational field, indicating that the direction of the resultant specific force, i. e., the apparent vertical, is the vector resultant of the gravitational specific force and the inertia reaction specific force.



Pendulous Element Seeks to Align its Pivot - Center of Mass Separation with the Resultant Specific Force.

Fig. 1-2 Specific forces acting on a pendulous element.

To obtain the specific forces acting on a pendulous element during a navigational problem, it is necessary to know the associated accelerations. The linear acceleration of a point with respect to a reference coordinate system may comprise five components with respect to a coordinate system that is moving relative to the reference coordinate system. However, as far as marine navigation is concerned, only two components are significant.

1. The tangential (horizontal) acceleration associated with the angular acceleration of the true vertical as the vehicle accelerates over the Earth's surface.

2. The centripetal acceleration parallel to the projection of the Earth-radius on the equatorial plane, due to the Earth's daily rotation; this, added to the gravitational field intensity, gives the gravity field intensity.

When a vehicle moves over the nearly spherical earth, the vertical associated with its instantaneous position rotates approximately geocentri-

cally with respect to the Earth. On a ship moving at constant speed along a great circle over the Earth, a pendulum would have to rotate with respect to the Earth at an effectively constant angular velocity in order to indicate the vertical continuously. Once the transient stages were over, no torque would be required to keep the pendulum along the vertical during this rotation. If the vehicle were to accelerate, by changing either speed or heading, a torque would be required to maintain the pendulum on the vertical, which in turn would be geocentrically accelerating.

Schuler ⁽¹²⁾ pointed out in 1923 that accurate indication of the vertical during periods of acceleration could be realized by suitable tuning of the natural period of the pendulum. Whenever the pivot of a pendulum is accelerated, the center of mass of the pendulum tends to lag behind the pivot with respect to inertial space. At the same time, this acceleration causes the true vertical, associated with the pivot, to accelerate geocentrically with respect to inertial space. These considerations lead to the following observation:

If a pendulum initially hangs vertically, it will remain along the vertical if its angular acceleration about its pivot equals the geocentric angular acceleration of the vertical. (The accelerations are with respect to inertial space.)

These two accelerations become equal for a distributed-mass pendulum when the ratio of the pivot-center of mass separation to the square of the radius of gyration of the pendulum equals the reciprocal of the radius of the Earth. When operation is in the Earth's gravity field, and the pendulum is undamped, this condition gives a pendulum with a natural period of approximately 84 minutes. For a shorter-period pendulum the rotation-producing torque on the pendulous element is stronger, so the pendulum lags the true vertical. For a longer-period pendulum the torque is weaker and the pendulum leads the true vertical.

An 84-minute period is very long compared to the periods of physical pendulums ordinarily encountered. In fact, it is improbable that a simple (concentrated-mass) pendulum or a distributed-mass pendulum could be constructed with this period, although the 84-minute gyropendulum just fails of being realizable. However, in the practical case, a condition analogous to the Schuler-tuning of a pendulum can be realized in a particular kind of closed-loop system in which a short-period pendulum tracks the

the specific forces. A platform, controlled on the basis of the pendulum output data, then becomes an equivalent Schuler pendulum.

From the foregoing, it is deduced that a vertical indicating system is conceivable which, while not a pendulum, utilizes the Schuler-tuning idea, so that a torque caused by the vehicle's acceleration acting on the system will be absorbed by the inertia reaction torque required to keep a reference line in the system on the vertical.

Reference (15), from which the foregoing section was obtained, has elaborated upon this theory and set forth six representative inertial systems for position indication.

Fundamentals of Position Indication

Astronomical position measurement involves the determination of the essentially geocentric angles between indicated and reference verticals. It is proposed to determine these angles by using a stabilized platform as an essential feature. The stabilization loop receives specific force data from accelerometers or pendulums, and delivers these data to gyro units and servo drives, which in turn drive the platform toward a horizontal position. The specific force data are modified and filtered to control the system dynamics. Part of this modification consists of Schuler-tuning the stabilization loop. Two basic methods of utilizing the indicated vertical are then available to obtain the vehicle's essentially geocentric angle of travel. One, called here analytical integration, involves the integration of accelerometer outputs or of gyro inputs, with the accelerometers and gyro units mounted on the stable platform. The other method, called here geometric integration, involves the direct comparison of the indicated vertical with a reference vertical. Both methods have been outlined⁽¹⁴⁾ in terms of six representative systems utilizing ideal components and undamped systems, namely:

- (1) Open-Chain Integration of the Angular Velocity of the Indicated Vertical.
- (2) Open-Chain Double Integration of the Angular Acceleration of the Indicated Vertical.
- (3) Direct Double Integration of Acceleration.
- (4) Electromagnetic Composition of Tangential and Vertical Components of Celestial Longitude Rate.

- (5) Geometric Integration Using Angular Velocity of the Indicated Vertical with Respect to Inertial Space.
- (6) Geometric Integration Using Pre-aligned Inertial Reference.

The first system will now be considered in some detail using nonideal components in both the damped and undamped systems, with special emphasis on the problem of determining a possible method for setting up performance specifications for components. It should be noted here that the normal methods of frequency analysis do not apply directly where the system does not reach steady state during its normal operating cycle, or where the transient period of the system is of primary interest. Such is the case in the operation of an inertial position indication system.

Open-Chain Integration of the Angular Velocity of the Indicated Vertical

Figure 1-3 is a functional diagram of a single-degree-of-freedom system for indicating the vertical. Figure 1-4 is a functional diagram of the essential operating components of a latitude indicator which uses an open-chain single integration of the angular velocity of the indicated vertical to arrive at the indicated latitude. Figure 1-4 corresponds to Fig. B-1 in Appendix B. Note that Fig. B-1 is primarily the basic vertical indicator of Figs. A-3 and 1-3, with the angular velocity integration tapped off the vertical indicator loop at the angular velocity signal that calls for precessing the gyro unit, so that the position integrator output is the indicated change in latitude. The vertical indicator is undisturbed by the presence of this integrator, as far as the loop dynamics are concerned. Hence, the same Schuler-tuning conditions apply to this system as applied to the basic vertical indicator of Fig. A-3.

A two-degree-of-freedom system constructed along these lines would require an x-axis accelerometer in addition to the y-axis accelerometer shown in Fig. 1-4, as well as x-axis components corresponding to the orientational control-signal generating system, gyro unit, and controlled member drive. In addition, the x-axis system requires that its angular velocity signal be modified by secant of latitude, in order to give longitude rate data to its position integrator. The position integrator in the x-axis system would indicate longitude difference with respect to some arbitrary reference. The maintenance of the y- and x-axes along a parallel of latitude and a meridian respectively must be handled by an auxiliary orientation system, e. g., a gyrocompass. (15)

The gyro units ideally maintain their spin axes fixed with respect to inertial space. To maintain the controlled member on which they are mounted tangential to the Earth in its daily rotation therefore, the x-axis gyro must be precessed by a correction torque that keeps the platform up with Earth rate. The calculations of Appendix B consider this torque to be generated by a special precession current applied to the torque generator of the gyro unit.

In Appendix B, it is shown that, if the controlled member has the equation of motion of a Schuler-tuned pendulum, the correction to the indicated position (that is, the instantaneous difference between the true and indicated positions) has a similar equation of motion, except for the appearance of certain initial conditions as additive constants of integration in the indicated position. Specifically, the correction to the indicated position at any time is the correction to the indicated position at the start of the problem, plus the present correction to the indicated vertical. The indicated position is thus Schuler-periodic with respect to boundary-matching terms associated with the vertical indication. The above description holds directly with ideal components throughout the system. Position indication will be modified somewhat however, where uncertainties are present in the system, as is shown in Appendices A and B.

CHAPTER 2

PROPOSED METHOD FOR ARRIVING AT COMPONENT SPECIFICATIONS UNCERTAINTIES IN COMPONENTS

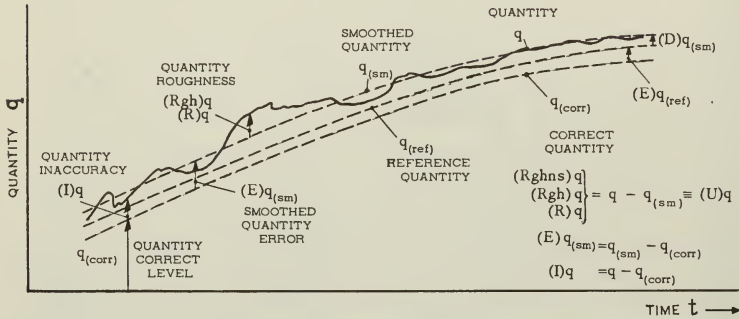


Fig. 2-1 Graphical definitions of inaccuracy, roughness, and error, for a quantity varying with time.

Figure 2-1 is a graphical definition, by Draper ⁽³⁾, of inaccuracy, roughness, and error for a quantity varying with time. The relationships shown are summarized below for convenience.

$$(R)q = (U)q = q - q_{(sm)} \quad (2-1)$$

$$(E)q_{(sm)} = q_{(sm)} - q_{(corr)} \quad (2-2)$$

$$(I)q = q - q_{(corr)} \quad (2-3)$$

$$= (U)q - (E)q_{(sm)} \quad (2-4)$$

also

$$(C)q_{(sm)} = -(E)q_{(sm)} \quad (2-5)$$

In the remainder of this thesis, when the error and correction in q are referred to, it will be taken to mean $(E)q_{(sm)}$ and $(C)q_{(sm)}$.

The ideal components used in the inertial systems described in Report R-9 ⁽¹⁴⁾ have been replaced, for the purpose of this study, with components which are no longer ideal in that the individual components now are considered as introducing spurious signals into the system by their operation.

For the purposes of this study, uncertainty in the output of an integrator has been treated as an equivalent spurious input to the integrator ⁽¹¹⁾. The specifications for an integrator in which the process has no specified maximum value may be written:

$$(U)q_{(out)(int)} \leq \frac{S_{(int)}}{N} \int_0^t q_{(in)(spec)} dt. \quad (2-6)$$

That is, the specification is such as to require that the uncertainty of the output quantity of the integration process be less than a percentage of the magnitude of the integral of some specified value of the input quantity to the integrating system, over the interval of integration. In this connection, it must be assumed that the uncertainty of the integration process will not be truly random over the period of integration because of the fact that the integrator may be subject to inaccuracies, such as drift and frictional losses, which do not lend themselves to correction; therefore, the average uncertainty of the integrating process will be different from zero over the period of integration. Similarly, the uncertainty in the output of an amplifier may not be a truly random process over a given interval because of amplifier drift, and the average uncertainty will therefore be different from zero over the interval. From the foregoing, it appears that specifications similar to those placed upon the integrator may be placed upon the amplifier, i.e., that the uncertainty in the output shall be less than some percentage of the magnitude of the output due to a specified value of the input quantity taken over a specified period of time.

The foregoing may be represented mathematically as in Equation (2-7) where

$$(U)q_{(out)(amp)} \leq \frac{S_{(amp)}(q_{in}, q_{out})}{N} q_{(in)(spec)}, \quad (2-7)$$

or its equivalent

$$(U)q_{(out)(amp)} \leq \frac{q_{(out)(spec)}}{N} \text{ over the specified time interval.}$$

It should be noted that, in both the integrator and the amplifier, the specification implies that the input signal has undergone an ideal integration or amplification, and that superimposed upon the output is an inaccuracy which is due wholly to an uncertainty; specifically, that the processes of integration and amplification are carried through without error. Uncertainties in gyro units and controlled member drives, pendulum units, and accelerometer units as developed by the Instrumentation Laboratory are generally susceptible to separation into two categories: those due to uncertainties in electronic signals applied as inputs to the torque summing member or derived as outputs from the position of the torque summing member; and those due to torque uncertainties acting on the torque summing member, such as mechanical unbalances, bearing friction, and undesirable reaction torques applied to the torque summing member by the microsyn signal units, etc. The subject has been treated extensively in several references,(10), (7), (6), and (16), and is of such scope that no attempt will be made to analyze it here, beyond the general observation that the results of open-chain tests would seem to indicate that the powerful methods of statistical analysis might be necessary in order to determine the suitability of units of various designs for inertial system applications. This method, which is essentially that recommended in later sections, again would treat the units as ideal, with uncertainties superimposed on the output of the ideal unit; hence, preliminary specifications may be laid down following principles to be developed later.

In the previous section, uncertainties are defined, and the manner in which uncertainties may arise in various components are discussed. Now, it is necessary to consider the effect of uncertainties when the components from which they arise are employed in closed-loop systems. In particular, performance of components in a closed-loop system, as for instance the vertical indicating loop of Fig. 1-3, affects the dynamics of the loop, thereby determining the precision of indicating the vertical. Components which operate in open-chain fashion outside the loop, as for instance the position indicating integrator of Figs. B-1 and B-2, have direct additional effects on the precision of the system. Hence, the open-chain specification method, as proposed in previous paragraphs, as well as the method for arriving at performance specifications for closed-loop components, is of direct application.

By the assumption that $q_{(in)}$ is operated on by a particular component ideally, but that the component itself then contributes an uncertainty in the output which is superimposed upon the true output, we have in effect separated the total output into the sum of two outputs, one of which is the true output, and the other, the portion of the total output due to the uncertainty. If, then, it were possible to predict by some simple means the magnitude of the uncertainty and the way in which it varies with respect to some variable, say time, then it should also be possible to determine what effect the uncertainty would have upon the performance of the system.

Unfortunately, the very term uncertainty implies the nature of the difficulty. We cannot by any simple means determine the necessary information on the behavior of the uncertainties. However, by statistical study of the behavior of components under various operating conditions, it may be possible to determine the probable form of the uncertainties. In this report, it is considered that the results of such a study would be presented in the form of power spectral densities, which would then be used to enter the response curves for a given system, in order to determine the effect on system performance of a component with an output uncertainty of a certain spectral density.

Since, in a position indication system, we are dealing with a dynamical system of second-order or higher, and, since our systems are lightly damped, the system may have normal modes or resonant frequencies that can be excited by forcing functions of the same frequency. In particular, Wrigley has shown ⁽¹³⁾ that an undamped vertical indication system of the type described later in this thesis is insensitive to a forcing function with an 84.4-minute period.

The mathematical expression of the weighting function describes these modes, which are found to be the terms of the form $t^k e^{p_1 t}$ into which the weighting function can be broken. ⁽⁹⁾ In a complicated system, it may be very difficult to obtain an explicit mathematical statement for $W(t)$, and, in design problems, the amount of work involved in optimizing system parameters for the presence within the system of certain exciting frequencies may be excessive. A further discussion of the weighting function is included in later sections. On the other hand, as shown in Appendix D, it may be a relatively simple matter, using machine methods, to determine the steady-state transfer function, $Y(j\omega)$, the weighting function and the transient transfer function, $F(\omega, t)$, which is defined and discussed later; and from these to con-

struct charts from which system specifications can be prepared.

The purpose of the following sections is to present in detail the manner in which such information may be utilized either in preparing specifications or in predicting the performance of the system.

Again, it should be emphasized that the necessity for evaluating position information at all times the system is in operation requires a detailed consideration of the transient which persists for a considerable length of time because of the long natural period of the system, and the long system characteristic time.

THE TRANSIENT TRANSFER FUNCTION

Consider some arbitrary system performance function that may be represented

$$\frac{q(\text{out})}{q(\text{in})} = \frac{(p + b_0)}{p^3 + a_2 p^2 + a_1 p + a_0} \quad (2-8)$$

The transfer function $Y(p)$ is frequently defined as the expression on the right with initial conditions zero, which is also the Laplace transform of the weighting function, where the weighting function is defined as the response of the system to a unit impulse with the system initially at rest.⁽⁹⁾

In the usual frequency response studies of a dynamical system, the steady-state response to a periodic function is the item of interest. In an inertial navigation system, however, because of the long system periods involved, the system may and probably will be placed in use before the steady-state has been achieved. Furthermore, the effects of system disturbances are present as transients for such a length of time that a study of the transient response of the system to periodic forcing functions appears necessary.

In order to study this transient response, we will define a new parameter such that, if a system represented by a performance function of the form of Equation (2-8) is subjected to a forcing function of the form $\cos wt + j \sin wt = e^{j\omega t}$, the response may be represented as follows:

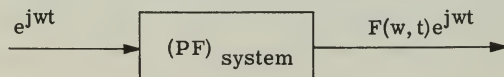


Fig. 2-2. System performance function.

where, for the steady-state, $\lim_{t \rightarrow \infty} F(w, t) \rightarrow Y(w)$, the transfer function for the system in which $Y(w)$ will now be defined as the steady-state response of the system to the forcing function $e^{j\omega t}$. The $F(w, t)$ then represents the transfer function of the system during the transient portion of the response, and is the parameter in which we are interested; moreover, it may be obtained by subjecting the system, initially at rest, to forcing inputs of the form $e^{j\omega t}$ for a series of frequencies and obtaining the time response of the system. $|F(w, t)|^2$ thus obtained may be plotted vs. time for various frequencies. From these plots, cross plots of $|F(w, t)|^2$ for various times vs. frequency can also be prepared (Fig. 3-17). The manner of obtaining $|F(w, t)|^2$ is of interest and is covered in Appendix (D).

Now, postulating that any disturbance to which the system is likely to be subjected can be assigned a power spectral density $G(w)$, we may write for the steady-state: ⁽⁹⁾

$$G_{(out)}(w) = |Y(w)|^2 G_{(in)}(w). \quad (2-9)$$

Analogously, for the transient period,

$$G_{(out)}(w, t) = |F(w, t)|^2 G_{(in)}(w). \quad (2-10)$$

Further, it can be shown that the ensemble mean square value of the output quantity at any time t_1 , for any arbitrary input with power spectral density given by $G_{(in)}(w)$, is the integral of the product of the spectral density of the input and the square of the transient transfer function at time t_1 between the limits $w = 0$ to $w = \infty$, that is,

$$\text{MS output at time}(t_1) = \int_0^{\infty} |F(w, t_1)|^2 G_{(in)}(w) dw. \quad (2-11)$$

It should be pointed out here that the ensemble mean square may be defined as the mean of the squared end-point values of $q(t)$ at time t_1 , for a number of trials; whereas the time mean square commonly used in communications applications is the time averaged mean square of $q(t)$ over a specified time interval. Since we are interested in the output of our system at any specified time rather than the average output over some arbitrary time interval, it follows that the ensemble mean square of the output is the quantity of interest.

Now supposing $|F(w, t)|^2$ to be determined by some such means as that described in Appendix (D); a plot might then be constructed presenting

$|F(w, t)|^2$ vs. frequency, as shown in Fig. 3-18. It will be noted that by using this plot, and assuming that $G_{(in)}(w)$ may be represented as a constant, the integration of Fig. 3-17 could be performed as the product of $G_{(in)}(w)$ and the area under the curve of $|F(w, t)|^2$. Or more generally, given plots of $|F(w, t)|^2$ and spectral density of a forcing function $G_{(in)}(w)$ vs. w for any system under consideration, neither curve being necessarily representable analytically, where $|F(w, t)|^2$ is plotted for time t_1 and spectral density is time invariant, the integration of Equation (2-11) may be performed by any of several standard methods of graphical integration. (14)

An examination of Fig. 3-18 reveals that the open-chain uncertainty specifications previously discussed are insufficient to specify component performance in a closed-loop system, since no account is taken of possible frequency components present in the uncertainties. Fig. 3-18, for example, shows that frequency components in the vicinity of $FR = 1$ will have far greater effect than, for instance, the same magnitude of uncertainty with frequency components in the vicinity of $FR = 4$. However, by making certain assumptions, it is possible to use the information obtained from a study of $|F(w, t)|^2$ to arrive at preliminary component specifications.

If the uncertainty output of a component is assumed to be a purely random process, i. e., the uncertainty has the characteristic of "white noise", the power spectral density of the uncertainty is then constant over an infinite band of frequencies from zero to infinity. However, $|F(w, t)|^2$ may approach zero if the system with which it is associated has an upper cut-off frequency, that is, input frequencies beyond a certain upper value of frequency will have no discernible effect on the system output. All the systems considered in this report have this upper frequency cut-off characteristic, i. e., the systems behave as low-pass filters, and the assumption of "white noise" may therefore be of use.

It should be noted, however, that an assumption of "white noise" of a given amplitude, is one of the worst which can be imposed upon a system, since the integration then involves all frequencies with equal weight. It seems reasonable to assume that the actual operating component will give rise to uncertainties whose frequencies will be predominantly centered within certain frequency bands, with negligible components outside these bands. If then the maximum spectral density in the predominant bands were to be applied to the system as "white noise" of the same amplitude, the resulting system performance would be worse than the actual by the

value of the integral outside the predominant frequency bands.

The above reasoning suggests that preliminary specifications might be written on the basis of the open-chain performance specifications if it is assumed that the uncertainties thus obtained are the worst possible "white noise" cases. Then, any improvement which might occur because of more favorable frequency distributions may be considered as a welcome gratuitous improvement in system performance.

System specifications for position indicating systems are generally written as requiring that indicated position be within specified limits of true position during specified time limits. The procedures of the foregoing yield information on the mean-square errors in system indication due to uncertainties in individual components. It can be shown that the sum of the magnitudes of these individual mean-square errors is equal to the mean-square error in the system output when due regard is given to the possibility that the individual terms may be complex. Hence, the procedure followed in the remainder of this report is to analyze the systems on the basis that each component in turn is nonideal, the remaining components in the system being considered perfect. The information thus obtained should be useful in evaluating which components contribute the most to system error, and in determining lower marginal requirements which must be met by components to be considered for use in the system.

THE WEIGHTING FUNCTION

The weighting function $(W(t))$ may be defined as the inverse transform of the term on the right of Equation (2-8). For further discussion of this subject, the reader is referred to any good text on servomechanisms. ⁽⁹⁾ ⁽²⁾ The weighting function for any system can be determined by subjecting the system to a unit impulse, i.e.,

$$W(t) = (PF)_{\text{system}} (u_1)t,$$

where

$$(u_1)t \equiv \text{unit impulse.}$$

Conversely, since the unit impulse is the derivative of the unit step, the weighting function is also the derivative of the response of the system to a unit step input.

The weighting function has the characteristic that it relates the previous inputs to the system to the present output by the integral

$$q_{\text{(out)}}(t) = \int_0^{\infty} q_{\text{(in)}}(t - \tau) W(\tau) d\tau, \quad (2-12)$$

where

$$\tau \equiv t - t_1 .$$

Hence, a knowledge of the weighting function enables one to form an estimate of the transient errors present in the output of the system following a forcing function which is applied over a given period of time and then goes to zero, such as the transient errors in an inertial system caused by maneuvers of the ship. This conclusion follows, if it is assumed that any given maneuver, occurring over a period of time, produces a forced error in the output of the system. If the ship then returns to a steady course and speed at time (t_1), the forcing function is no longer being applied to the system, but the error caused by the maneuver remains in the system at time (t) as a transient related to the forced error at time (t_1) by the value of the integral in Equation (2-12). The above example is a specialized application of the general theory by which a series of impulse or step functions may be used to approximate any arbitrary input to the system, and thus the normal response of the system to the input may be determined from the relationship of Equation (2-12).

CHAPTER 3

ANALYSIS OF VERTICAL INDICATORS

GENERAL

The differential performance equation for the position indicating system being considered in this thesis is derived in Appendix B. The differential performance equations for the associated vertical indicators, both damped and undamped, are derived in Appendix A. Equation (B-7) shows that the correction to the indicated vertical, $[(C)V]_{(t, i)}$, enters directly as one of the terms in the correction to the indicated position, $[(C)P]_{(t, i)}$. Consequently, in the future, when references are made directly to the performance of the vertical indicator, the reader may infer that reference to position indication is implied as well.

In this chapter, we will consider first the undamped vertical indicator, and finally the damped vertical indicator. The concept of a transient transfer function as introduced in Chapter 2 will be used as an aid in evaluating the effects of certain uncertainties upon the vertical indication. Since the results of any uncertainty spectral-density analyses on the various components have not been available to the authors, if indeed such studies exist in usable form, only qualitative estimates will be made as to the relative performances required of the various components.

UNDAMPED VERTICAL INDICATOR

Figure 3-1 presents in summary form the equations of $|F(w, t)|^2$ for the undamped vertical indicator. Figure 3-2 is a semi-log plot of Equations (3-5) and (3-6) vs. frequency ratio for a time of one-half hour. Photographs of transient transfer functions of damped vertical indicators are shown in Fig. 3-3. These damped systems are to be discussed later in this chapter. It will be recalled that the mean-square errors obtained in the proposed method are the ensemble mean squares, and consequently represent the errors at a particular instant of time. Further, by the previous definitions, the time interval is measured from the instant the forcing

Given the performance equation of a system for which the response to a forcing input of the form $e^{j\omega_f t}$ is desired, and recalling that $e^{j\omega_f t} = \cos \omega_f t + j \sin \omega_f t$, the response of the system to $e^{j\omega_f t}$ is given by the complex sum of the separate responses of the system to $\cos \omega_f t$ and $\sin \omega_f t$. We can apply the foregoing to the undamped vertical indicator with the differential equation (Eq. A-32), which may be written

$$[\ddot{x} + \frac{W_f}{W_{NB}}] [(O)W] (t, 1) = S_{(q_{(in)0}, 0)} q_{(in)0} + S_{(q_{(in)1}, 0)} \dot{q}_{(in)1} \quad (A-32)$$

where $q_{(in)1}$ and $\dot{q}_{(in)2}$ correspond to the appropriate quantities appearing in the zero and first order derivatives respectively of equation (A-32) in Appendix A.

Denote by $f_{(n)}(\cos)(t)$, the response of the system to $q_{(in)(n)} = \cos \omega_f t$ where the subscript (n) is the order of the derivative associated with $q_{(in)(n)}$, and by $f_{(n)}(\sin)(t)$, the response of the system to $q_{(in)(n)} = \sin \omega_f t$. Then taking initial conditions equal to zero, the solution for Eq. (A-32) to the forcing function $e^{j\omega_f t}$ may be written as the sum of the four terms below.

$$f_{(0)}(\cos)(t) = \frac{\cos \omega_f t - \cos \frac{W_f}{W_{NB}} t}{\frac{W_f}{W_{NB}} - \omega_f^2} \quad (3-1)$$

$$j f_{(0)}(\sin)(t) = j \left(\frac{1}{\frac{W_f}{W_{NB}} - \omega_f^2} \right) (\sin \omega_f t - \frac{W_f}{W_{NB}} \sin \frac{W_f}{W_{NB}} t) \quad (3-2)$$

$$f_{(1)}(\cos)(t) = \left(\frac{1}{\frac{W_f}{W_{NB}} - \omega_f^2} \right) (W_f \sin \omega_f t - \frac{W_f}{W_{NB}} \sin \frac{W_f}{W_{NB}} t) \quad (3-3)$$

$$j f_{(1)}(\sin)(t) = j \left(\frac{W_f}{\frac{W_f}{W_{NB}} - \omega_f^2} \right) (-\cos \omega_f t + \cos \frac{W_f}{W_{NB}} t) \quad (3-4)$$

Recalling the definition of $|F(w, t)|$, Chapter 2, and making appropriate substitutions following the method of Appendix D, we obtain

$$|F(w, t)|_{(0)}^2 = |f_{(0)}(\cos)(t)|^2 + |j f_{(0)}(\sin)(t)|^2 = \left(\frac{1}{\frac{W_f}{W_{NB}} - \omega_f^2} \right)^2 [(\cos \omega_f t - \cos \frac{W_f}{W_{NB}} t)^2 + (\sin \omega_f t - \frac{W_f}{W_{NB}} \sin \frac{W_f}{W_{NB}} t)^2] \quad (3-5)$$

$$|F(w, t)|_{(1)}^2 = |f_{(1)}(\cos)(t)|^2 + |j f_{(1)}(\sin)(t)|^2 = \left(\frac{1}{\frac{W_f}{W_{NB}} - \omega_f^2} \right)^2 [(W_f \sin \omega_f t - \frac{W_f}{W_{NB}} \sin \frac{W_f}{W_{NB}} t)^2 + (\cos \omega_f t - \cos \frac{W_f}{W_{NB}} t)^2] \quad (3-6)$$

In an analogous manner, the time solutions for the zero order term of the damped vertical indicator of Equation (A-38) may be written

$$f_{(0)}(\cos)(t) = \frac{-\frac{1}{\sigma_D^2}}{\left[\frac{W_f}{W_{NB}} + \left(\frac{1}{\sigma_D^2} \right)^2 \right] \left[(2DR)W_{NB} - \frac{1}{\sigma_D^2} \right] + W_{NB}^2 (1 - (DR)^2)} e^{-\frac{t}{\sigma_D}} + \left\{ \left(\frac{1}{\sigma_D^2} \right)^2 + W_f^2 \right\} \left[(W_{NB} - W_f)^2 + 4 W_{NB}^2 (DR)^2 W_f^2 \right]^{1/2} \cos(W_f t + A_1) \quad (3-7)$$

$$+ \frac{1}{W_{NB} \sqrt{1 - (DR)^2}} \left\{ \left[\left(\frac{1}{\sigma_D^2} - (DR)W_{NB} \right)^2 + W_{NB}^2 (1 - (DR)^2) \right] \left[W_{NB}^2 (2(DR)^2 - 1) + W_f^2 \right] + 4 W_{NB}^4 (DR)^2 (1 - (DR)^2) \right\}^{1/2} e^{-(DR)W_{NB} t} \sin(W_{NB} \sqrt{1 - (DR)^2} t + A_2)$$

$$f_{(0)}(\sin)(t) = \frac{W_f}{\left[W_f^2 + \left(\frac{1}{\sigma_D^2} \right)^2 \right] \left[(2DR)W_{NB} - \frac{1}{\sigma_D^2} \right] + W_{NB}^2 (1 - (DR)^2)} e^{-\frac{t}{\sigma_D}} + \left\{ \left(\frac{1}{\sigma_D^2} \right)^2 + W_f^2 \right\} \left[(W_{NB} - W_f)^2 + 4 W_{NB}^2 (DR)^2 W_f^2 \right]^{1/2} \sin(W_f t + A_1) \quad (3-8)$$

$$+ \frac{W_f}{W_{NB} \sqrt{1 - (DR)^2}} \left\{ \left[\left(\frac{1}{\sigma_D^2} - (DR)W_{NB} \right)^2 + W_{NB}^2 (1 - (DR)^2) \right] \left[W_{NB}^2 (2(DR)^2 - 1) + W_f^2 \right] + 4 W_{NB}^4 (DR)^2 (1 - (DR)^2) \right\}^{1/2} e^{-(DR)W_{NB} t} \sin(W_{NB} \sqrt{1 - (DR)^2} t + A_2)$$

$$\text{where } A_1 \equiv -\tan^{-1} \frac{W_f}{\sigma_D} - \tan^{-1} \frac{2(DR)W_{NB} W_f}{W_{NB} - W_f}$$

$$A_2 \equiv \tan^{-1} \frac{\sqrt{1 - (DR)^2}}{-DR} - \tan^{-1} \frac{W_{NB} \sqrt{1 - (DR)^2}}{\frac{1}{\sigma_D} - (DR)W_{NB}} - \tan^{-1} \frac{2W_{NB}^2 (DR) \sqrt{1 - (DR)^2}}{W_{NB}^2 (2(DR)^2 - 1) + W_f^2}$$

$$A_3 \equiv \tan^{-1} \frac{\sqrt{1 - (DR)^2}}{-DR}$$

The corresponding $|F(w, t)|_{(0)}$ for Equations (3-7) and (3-8) is not included here, but the reader can readily verify that the resulting function is somewhat complex, and that $|F(w, t)|_{(0)}$ is not a particularly well behaved function of the forcing frequency.

Fig. 3-1 Summary of time solution for vertical indicators.

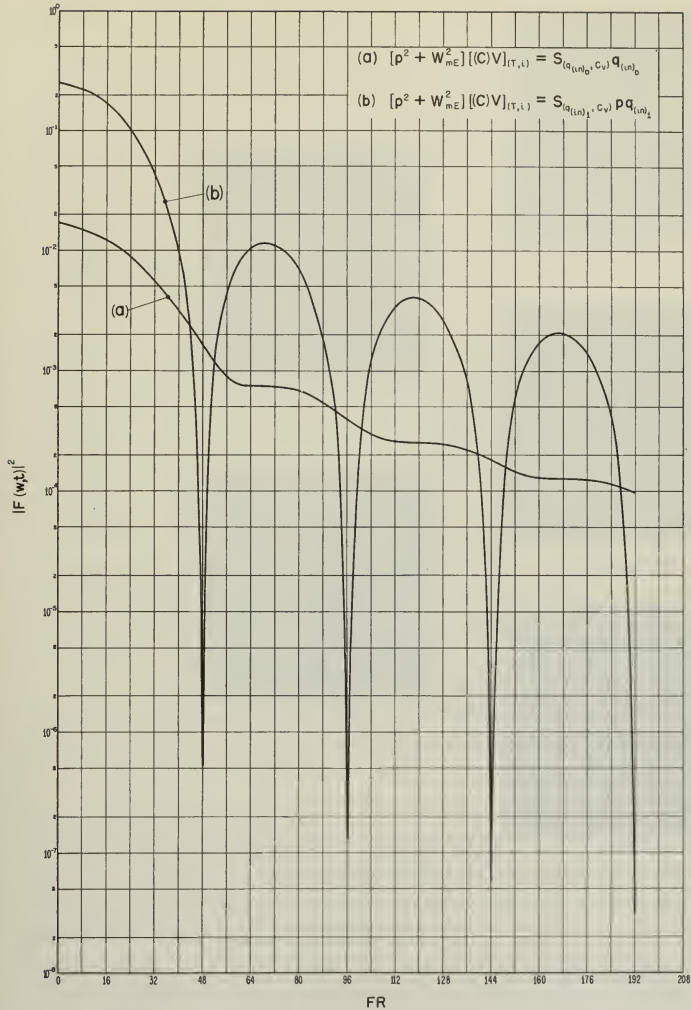
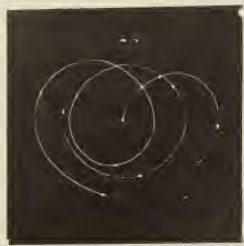


Fig. 3-2 Transient transfer function squared of undamped vertical indicator for time $t = 1/2$ hour.



(FR) = 1.91
(DR) = 0.3
Mag. 3.75x



(FR) = 1.43
(DR) = 0.3
Mag. 2x



(FR) = 0.95
(DR) = 0.3
Mag. 1x



(FR) = 1.91
(DR) = 0.5
Mag. 3.75x



(FR) = 1.91
(DR) = 0.1
Mag. 2.5x

$$\ddot{q}(\text{dep}) + \left(2(\text{DR})W_{ns} + \frac{1}{(\text{CT})_D} \right) \dot{q}(\text{dep}) + W_{ns}^2 q(\text{dep}) = W_{ns}^2 (W_{pe}^2 W_{pe}^2 t)$$

Fig. 3-3 Typical oscilloscope presentation of transient transfer function of damped vertical indicator.

function $e^{j\omega t}$ is applied to the instant in time under consideration. Also, although strictly speaking the frequency form of the transfer function is not defined for an unstable system ⁽⁹⁾, the frequency form of the transient transfer function does exist by the definition in Chapter 2.

The area under $|F(\omega, t)|_{(0)}^2$ plotted on linear coordinates would represent the integral $\int_0^\infty |F(\omega, t)|^2 G_{(in)}(\omega) d\omega$ with $G_{(in)} = 0$, $0 \leq \omega \leq \infty$, and is less than the area under the curve for $|F(\omega, t)|_{(1)}^2$ plotted in the same fashion. Hence, for "white noise" for which $G_{(in)}(\omega)$ is constant for all frequencies, the term containing the first derivative produces the greater error in vertical indication.

The first derivative term is associated with the uncertainty in gyro drift and with the inaccuracy in the speed compensation current. Conversely, the uncertainties in the accelerometer unit and the integrator within the vertical indication loop are associated with the zero-order term. Therefore, the performance of the gyro unit and the measurement of water speed will probably be more critical than the performance of the accelerometer unit and the integrator. This conclusion will be especially true if the spectral densities of the uncertainties have a wide band width such that the dips in $|F(\omega, t)|^2$ for the first-order term do not have an appreciable effect in reducing the associated errors.

The one-half-hour time was chosen as representative of possible situations in which a damped system would not be used. These situations would be those in which the period of operation would be short with respect to the time required to damp out transient disturbances, and hence no advantage would be gained from the greater complexity of the damped system.

DAMPED VERTICAL INDICATOR

Next, we consider the damped vertical and position indication system. The parameters used are those that provide the optimum position indication with respect to the angular velocity of the true vertical. The resulting parameters are summarized in Table C-I.

In Reference (8), the optimization was done on the opposite basis from that used in Appendix C; specifically, the acceleration error was eliminated and the jerk-error minimized. It is interesting to note that the attenuation of errors due to accelerations under the conditions of Reference (8) proceeds at 6 decibels per octave with increasing frequency, whereas

by using the present methods, acceleration errors are attenuated at 18 decibels per octave.

Figures 3-4 through 3-15 present, respectively, the steady-state sinusoidal responses of the vertical indicator, the step responses, and the impulse responses or weighting functions, for DR = 0.1, 0.3, and 0.5. As defined in Chapter 2, $|F(w, t)|$ is an analogous function to $|Y(w)|$, the transfer function; and hence the area under the curve of $|Y(w)|^2$ has the same utility for the steady-state as the area under the $|F(w, t)|^2$ has for the transient period. Hence, from a study of the steady-state response curves and a comparison with Equation (A-38), we may conclude, by reasoning similar to that applied in the case of the undamped system, that the uncertainties associated with the gyro unit and water-speed compensation will probably be most critical. Proceeding in a similar manner, we may arrive at the following listing, which is essentially a listing of components in direct order of the excellence of performance required, but without regard to the sensitivities which may be involved.

- (1) (a) Gyro unit
(b) Water-speed compensation
- (2) Accelerometer unit
- (3) (a) Direct-channel amplifier
(b) Earth-rate compensation
(c) Feedback amplifier
(d) High-frequency integrator
- (4) Low-frequency integrator

It should be noted that, in the damped vertical indication system, six sensitivities appear. These six sensitivities are related in Derivation Summary A-II by only four equations. Thus, we may impose two more conditions on the sensitivities, such that we arrive at six independent equations in the six sensitivities. It is apparent, then, that we may be afforded some leeway in adjusting sensitivities such as minimizing the errors due to some particularly objectionable component in the system.

No mention has been made in this chapter of the effect on position indication of uncertainties in the open-chain integrator. However, as shown in Appendix B, the mean-square error in position due to the open-chain integration may be developed in a manner analogous to that applied above.

The remainder of this chapter is devoted to a discussion of the methods

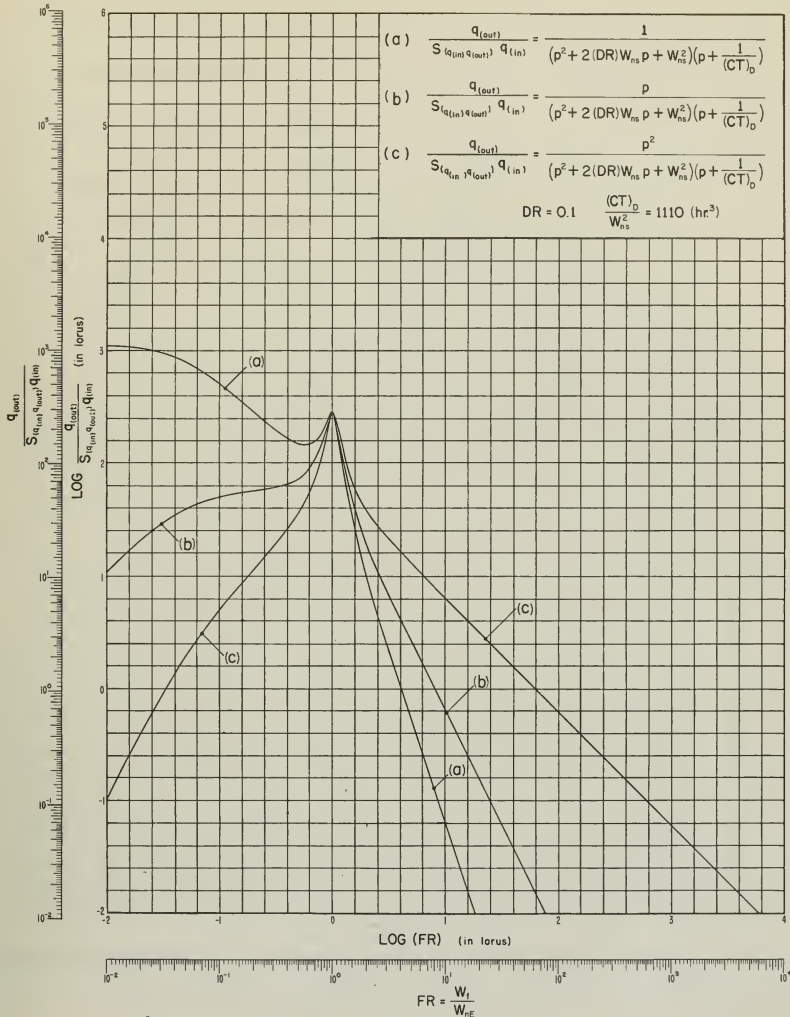


Fig. 3-4 Steady-state sinusoidal response of three subsystems of damped vertical indicator, DR = 0.1.

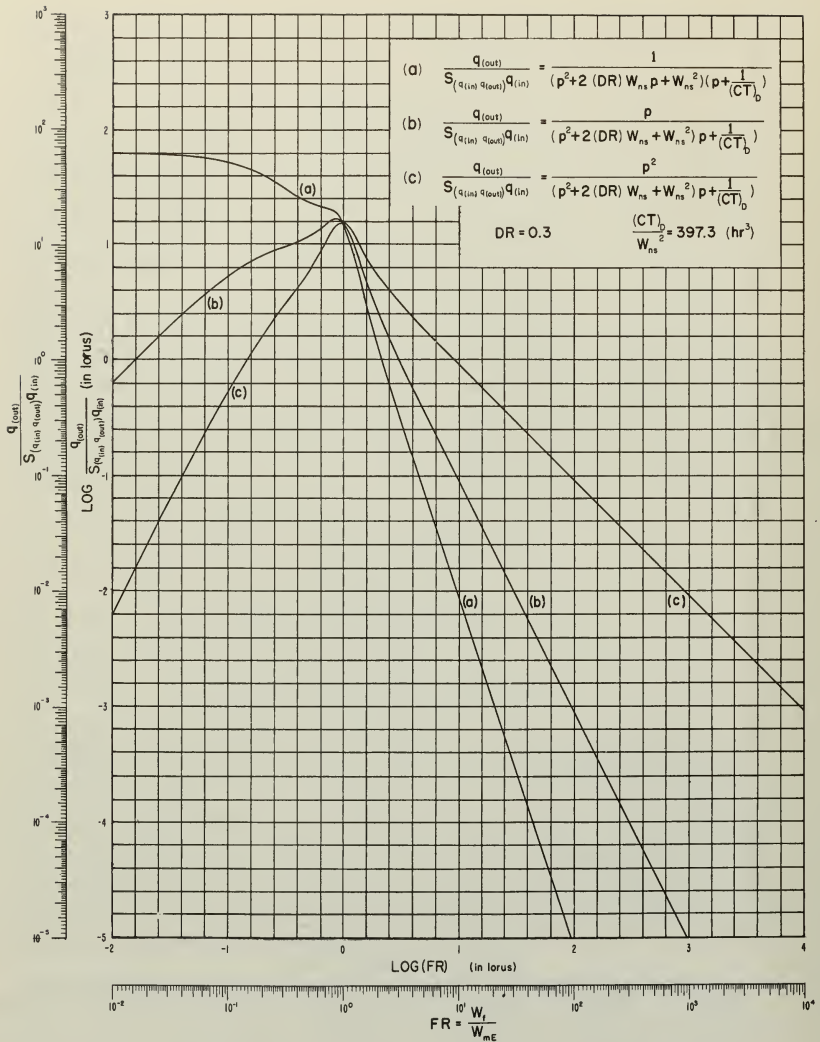


Fig. 3-5 Steady-state sinusoidal response of three subsystems of damped vertical indicator, DR = 0.3.

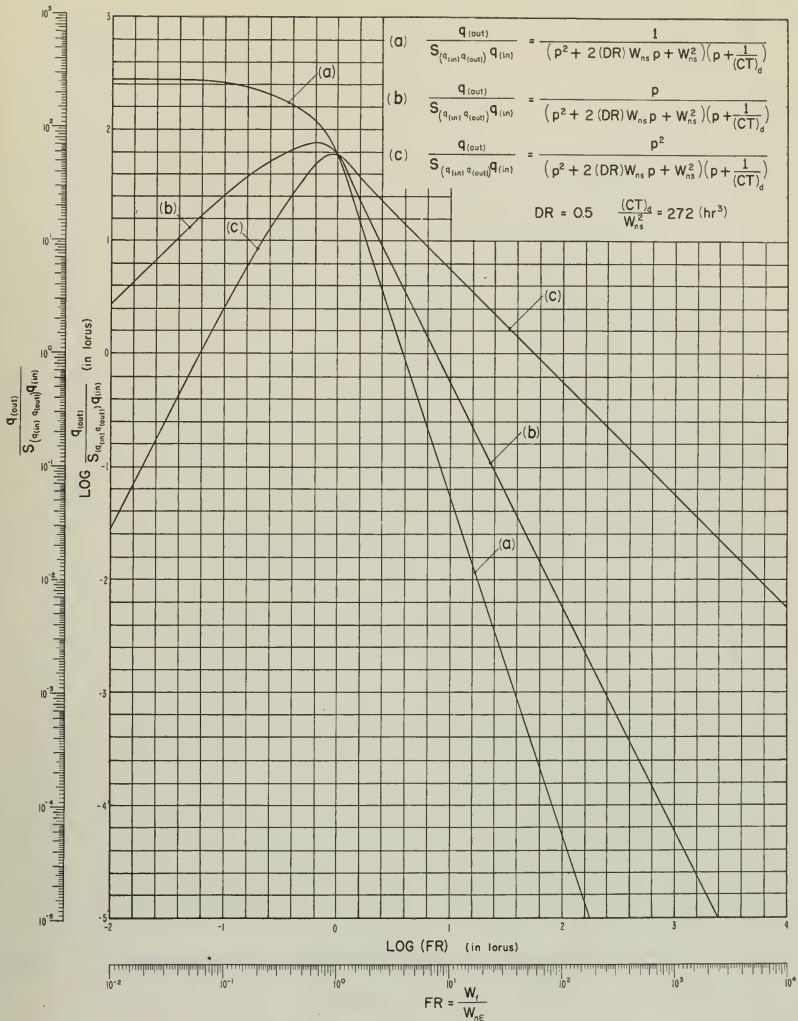


Fig. 3-6 Steady-state sinusoidal response of three subsystems of damped vertical indicator, DR = 0.5.

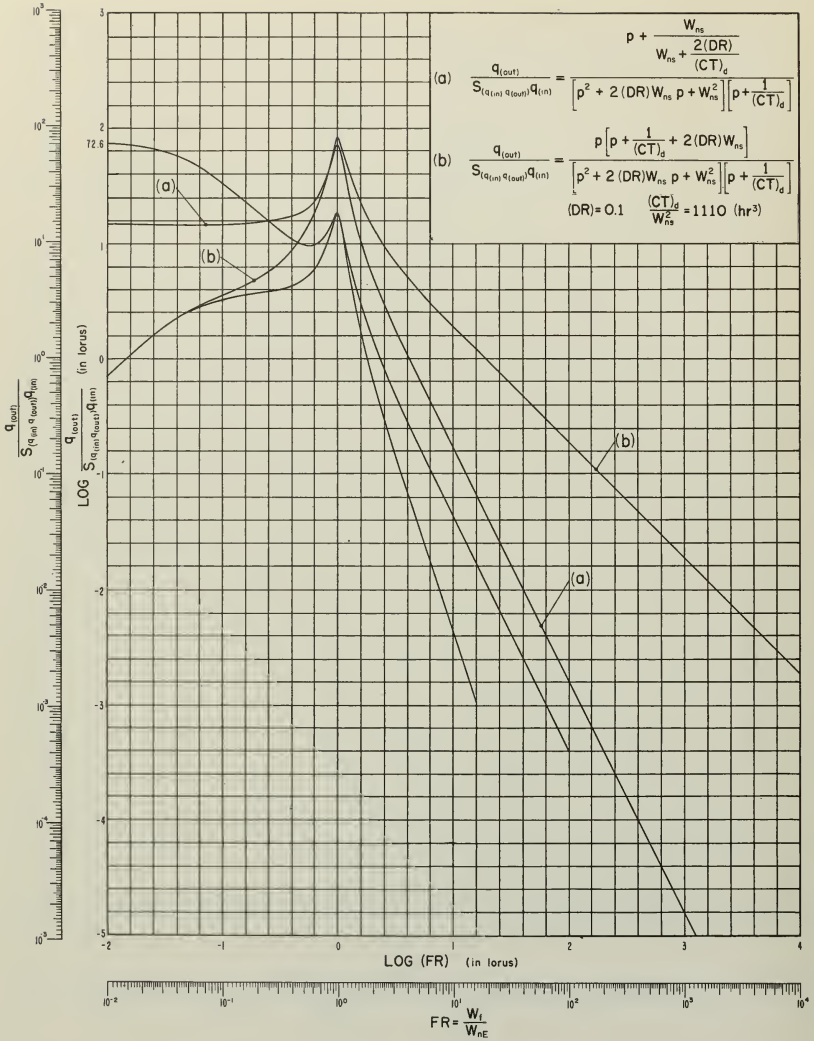


Fig. 3-7 Steady-state sinusoidal response of two subsystems of damped vertical indicator, DR = 0.1.

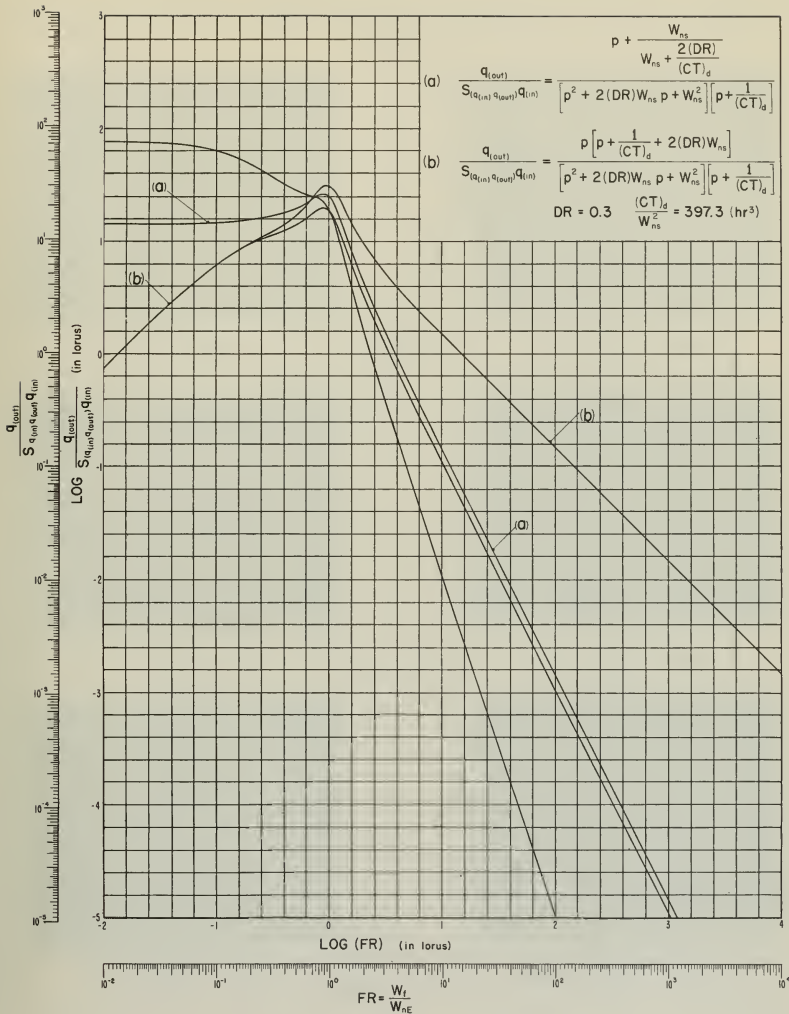


Fig. 3-8 Steady-state sinusoidal response of two subsystems of damped vertical indicator, DR = 0.3.

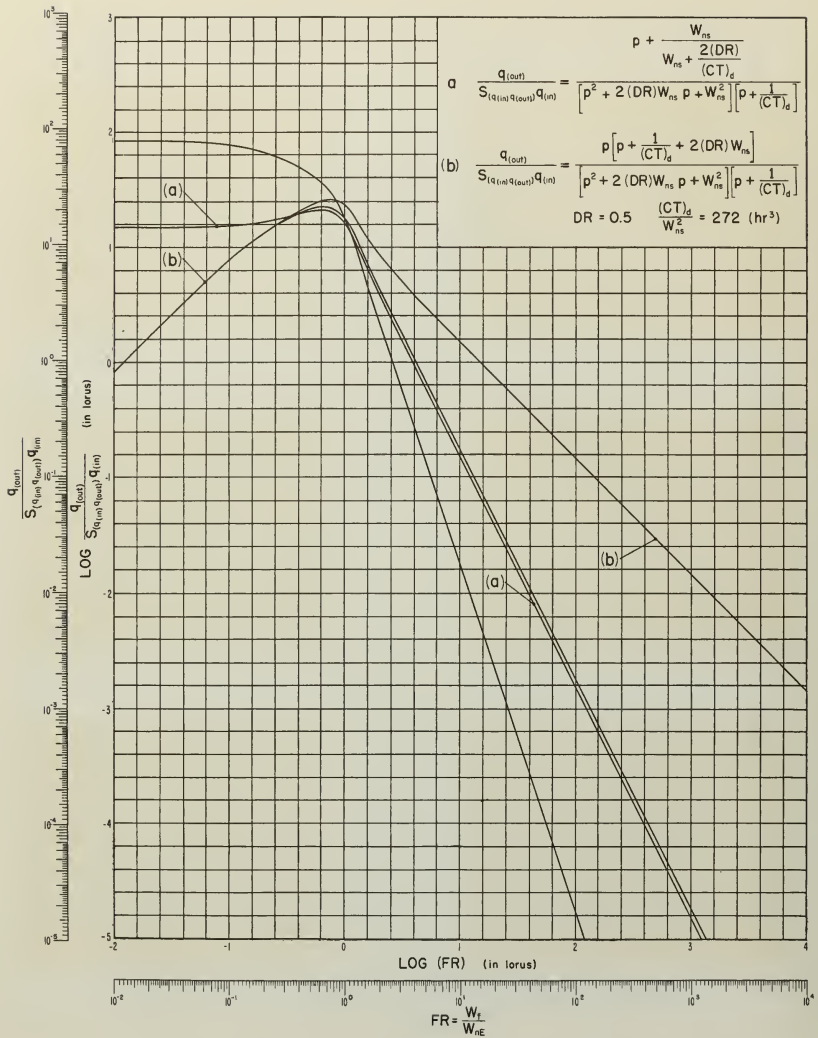
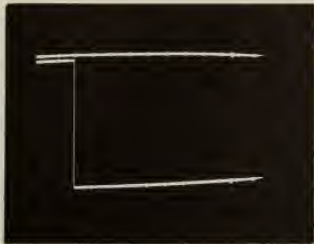
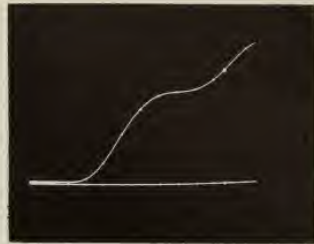


Fig. 3-9 Steady state sinusoidal response of two subsystems of damped vertical indicator, DR = 0.5.

$$[P] = p^3 + a_2 p^2 + a_1 p + a_0$$



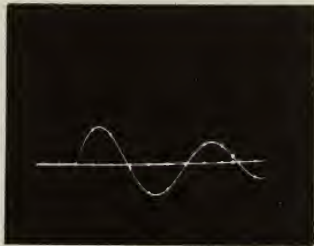
STEP INPUT



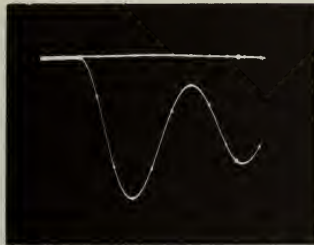
$$[PF] = \frac{1}{[P]} \quad \text{Mag. } 0.1x$$



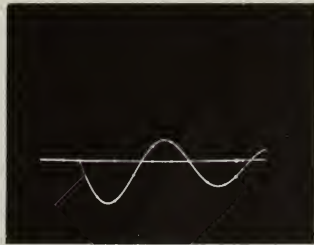
$$[PF] = \frac{p}{[P]} \quad \text{Mag. } 1x$$



$$[PF] = \frac{p^2}{[P]} \quad \text{Mag. } 1x$$



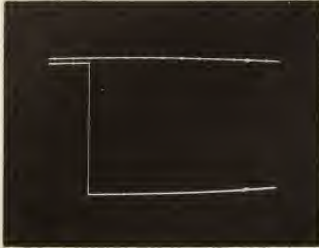
$$[PF] = \frac{p + a_0}{[P]} \quad \text{Mag. } 1x$$



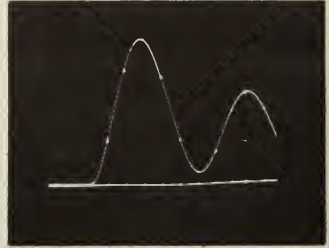
$$[PF] = \frac{p(p + a_2)}{[P]} \quad \text{Mag. } 1x$$

Fig. 3-10 Step response of damped vertical indicator, DR = 0.1.

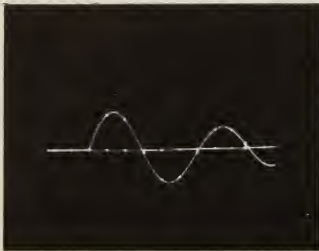
$$[P] = p^3 + a_2 p^2 + a_1 p + a_0$$



STEP INPUT



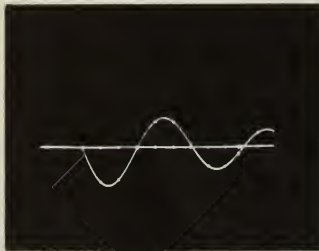
$[PF] = \frac{1}{[P]}$ Mag. 1x



$[PF] = \frac{p}{[P]}$ Mag. 1x



$[PF] = \frac{p^2}{[P]}$ Mag. 1x



$[PF] = \frac{p + \frac{a_0}{a_1}}{[P]}$ Mag. 1x



$[PF] = \frac{p(p + a_2)}{[P]}$ Mag. 1x

Fig. 3-11 Impulse response of damped vertical indicator (derivative of step response), DR = 0.1.

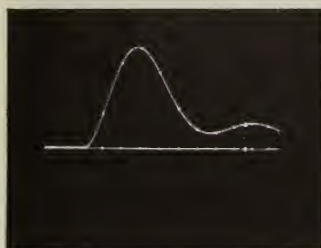
$$[P] = p^3 + a_2 p^2 + a_1 p + a_0$$



STEP INPUT



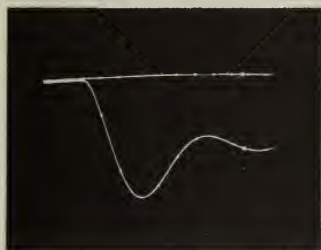
$$[PF] = \frac{1}{[P]} \quad \text{Mag. } 0.1x$$



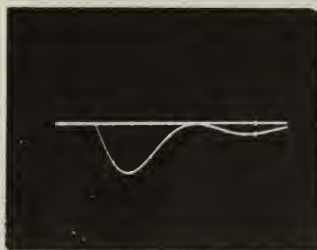
$$[PF] = \frac{p}{[P]} \quad \text{Mag. } 1x$$



$$[PF] = \frac{p^2}{[P]} \quad \text{Mag. } 1x$$



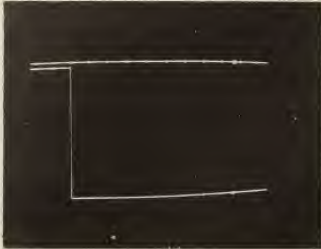
$$[PF] = \frac{p + \frac{a_0}{a_1}}{[P]} \quad \text{Mag. } 1x$$



$$[PF] = \frac{p(p + a_2)}{[P]} \quad \text{Mag. } 1x$$

Fig. 3-12 Step response of damped vertical indicator, DR = 0.3.

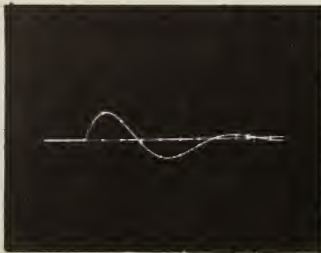
$$[P] = p^3 + a_2 p^2 + a_1 p + a_0$$



STEP INPUT



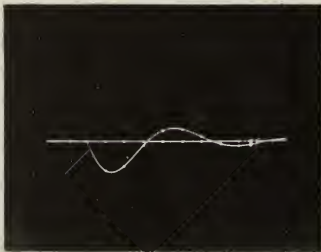
$$[PF] = \frac{1}{[P]} \quad \text{Mag. } 1x$$



$$[PF] = \frac{p}{[P]} \quad \text{Mag. } 1x$$



$$[PF] = \frac{p^2}{[P]} \quad \text{Mag. } 1x$$



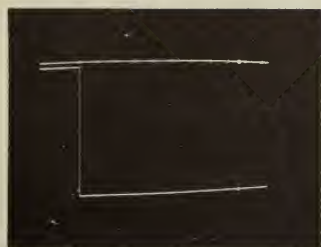
$$[PF] = \frac{p + \frac{a_0}{a_1}}{[P]} \quad \text{Mag. } 1x$$



$$[PF] = \frac{p(p+a_2)}{[P]} \quad \text{Mag. } 1x$$

Fig. 3-13 Impulse response of damped vertical indicator, (derivative of step response), DR = 0.3.

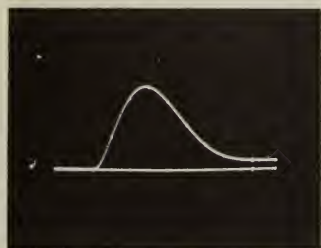
$$[P] = p^3 + a_2 p^2 + a_1 p + a_0$$



STEP INPUT



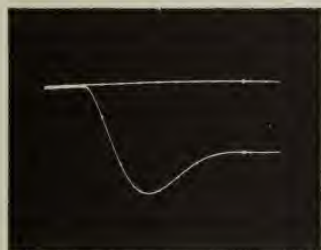
$$[PF] = \frac{1}{[P]} \quad \text{Mag. } 0.1x$$



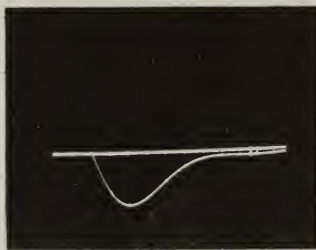
$$[PF] = \frac{p}{[P]} \quad \text{Mag. } 1x$$



$$[PF] = \frac{p^c}{[P]} \quad \text{Mag. } 1x$$



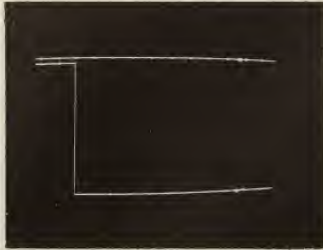
$$[PF] = \frac{p + \frac{a_0}{a_1}}{[P]} \quad \text{Mag. } 1x$$



$$[PF] = \frac{p(p + a_2)}{[P]} \quad \text{Mag. } 1x$$

Fig. 3-14 Step response of damped vertical indicator, DR = 0.5.

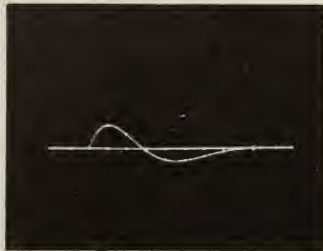
$$[P] = p^3 + a_2 p^2 + a_1 p + a_0$$



STEP INPUT



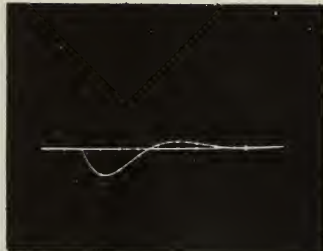
$$[PF] = \frac{1}{[P]} \quad \text{Mag. } 1x$$



$$[PF] = \frac{p}{[P]} \quad \text{Mag. } 1x$$



$$[PF] = \frac{p^2}{[P]} \quad \text{Mag. } 1x$$



$$[PF] = \frac{p + a_0}{[P]} \quad \text{Mag. } 1x$$



$$[PF] = \frac{p(p + a_2)}{[P]} \quad \text{Mag. } 1x$$

Fig. 3-15 Impulse response of damped vertical indicator, (derivative of step response), DR = 0.5.

used and the results obtained in studying the transient transfer function for the damped vertical indicator.

For the study of the damped vertical indicator, it was attempted to apply the method described in Appendix D, using a high-speed, general purpose analog computer.

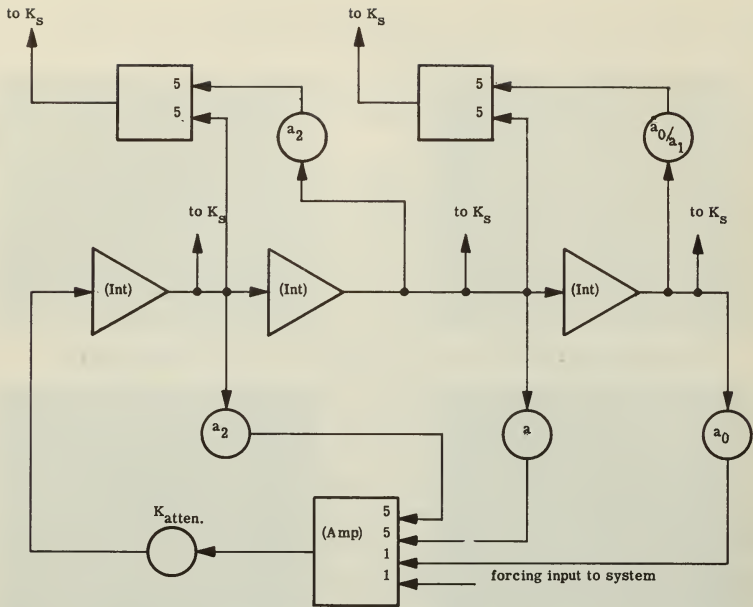
Two identical systems (Fig. 3-16a) were placed on the simulator and the forcing functions $\cos w_f t$ and $\sin w_f t$ were applied, one to each system. The output of one system was then taken to the x-axis of an oscilloscope. The resulting Lissajous pattern represented a plot of the sine response of the system vs. the cosine response, from which it was proposed to obtain the transient transfer function, $|F(w, t)|$.

It was intended that the sine and cosine functions be developed in an harmonic oscillator (Fig. 3-16b) as a part of the set-up. The oscillator would then oscillate at the frequency determined by the w_f setting when excited by a step input from the computer master generator.

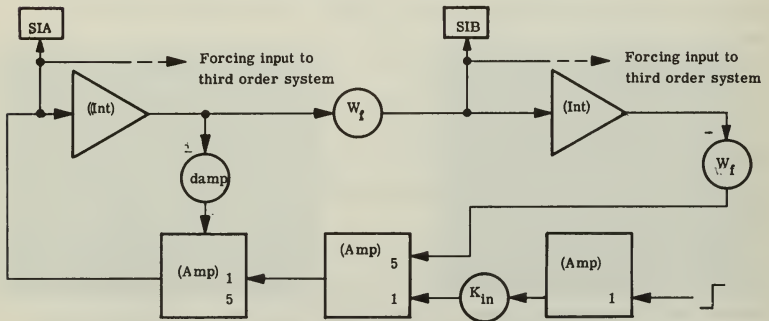
Theoretically, such an oscillator would be possible using an undamped second-order system, and the sine and cosine outputs plotted against each other would produce a circle on the oscilloscope. However, due to nonlinearities or other imperfections in the computer, it was found that the amplitude of the oscillations of both terms tended to change in magnitude. Consequently, it was found necessary to introduce either positive or negative damping into the system, depending upon the frequency, to maintain a constant amplitude.

The damping, in turn, affected the sine and cosine outputs differently; hence, it was necessary to include the "scope-attenuator" in each system to adjust the resulting ellipse to a circle. The use of an additional attenuator in this position will not introduce distortions in the system responses, since all signals are attenuated the same amount for a given setting.

The "input gain control" was put into the input to the harmonic oscillator to provide a calibrated gain control in order to increase or decrease the system responses to usable size. In tests, changes in setting of this control seemed to produce no distortion in the circular display of the sine vs. cosine pattern, and hence it may be assumed that the amplitudes of both were changed equally.



(a) Third order vertical indicator.



(b) Harmonic oscillator.

Fig. 3-16 Block diagrams of high-speed analog computer.

The remainder of the set-up is clearly apparent, the remaining gains and attenuators being applied merely to provide more reasonable potentiometer settings.

In calibrating the oscilloscopes, one of which was used as a monitor-scope, and the other as a photo-scope, the necessary damping ratio was first set into the harmonic oscillator. Then, with $K_{(in)}$ and K_S set to convenient values, the oscilloscope amplifiers were used to set in a two-inch diameter circle on the monitor-scope. Then, with $K_{(in)}$ reduced, and all other settings maintained constant, a two-inch circle was adjusted on the photo-scope using the oscilloscope amplifiers. The shift in $K_{(in)}$ in the calibrations was made so as to take advantage of the linear amplifiers on the oscilloscope to amplify small pictures, rather than alternatively applying large forcing signals with the attendant danger of distortion due to over-loading the computer.

After calibration, the oscilloscope amplifiers were left undisturbed. For each frequency thereafter, a two-inch circular plot of the sine vs. the cosine was obtained on the monitor-scope by manipulation of the damping ratio in the oscillator and the scope attenuators, K_S . The input gain was set at a convenient value for the above operation at each frequency and recorded, as was the gain used for photographing each response, in order that the responses might be reduced to a common reference. Calibration was completed by recording the two-inch, or unit-reference circle photographically, in order to provide a direct reference for reducing the data. Using the above methods, photographs of the Lissajous pattern responses of each of the sub-systems were made at various frequencies. It was apparent, however, that the highest forcing frequencies which might be applied corresponded to a frequency ratio of about five, because of the large attenuation in the system at higher frequencies and the consequent limitations imposed by the noise level in the computer. Thus the data could not be extended to the significant frequency region for which $FR > 16$. The data were then reduced from the Lissajous patterns, of which those shown in Fig. 3-3 are representative. The time dots on these patterns signify 4-hour intervals. An examination proved these data to be unreliable, since steady-state amplitudes thus obtained failed to agree with steady-state amplitudes computed by other means. As a consequence, no effort will be made to

present any quantitative results.

Alternatively, a qualitative summary of the results of a study of the Lissajous patterns from sub-system to sub-system and damping ratio to damping ratio is presented below. The points in the summary occur consistently and are considered significant in the transient study.

(a) An excursion of the response occurs that is greater than the steady-state response. In addition, the initial excursion may or may not be oscillatory.

(b) The response then returns toward the steady-state in an oscillatory manner, the frequency of the oscillations apparently increasing with increasing frequency.

(c) The ratio of the initial excursion to the steady-state response apparently increases with an increase in frequency.

(d) The time in hours at which the maximum excursion occurs is apparently a function of both damping ratio and frequency for any particular system, and, for the systems studied, varied from six to forty hours.

(e) The time of reaching the maximum excursion does not appear to be an orderly function of frequency for a particular damping ratio and system. That is, for increasing frequencies, the time at which the maximum excursion occurs may first show an increase and then a decrease. From the data obtained, no reliable conclusion seems possible as to the effect of damping ratio on the time for reaching the maximum excursion.

(f) The nature of the responses seems to indicate the inadvisability of designing a system purely on the basis of conventional steady-state analysis techniques, if the response during the transient period is of interest.

The previous statements are not considered by the authors to be a condemnation of the method. It is suggested that additional work, which could not be undertaken by the authors because of a combination of lack of time and non-availability of equipment, might yield interesting results. Conservatively, these results would show low-frequency behaviors of the sub-systems for the vertical indicator. It would then remain to determine the relationship, if any, that exists between the behavior at high and low frequencies.

A method proposed by Dr. J. H. Laning, Jr., of the Instrumentation Laboratory, Massachusetts Institute of Technology, would approximate the high-frequency transient transfer function using the response of the

system to impulses. This method will be investigated at some later date.

Another method, suggested by Dr. Sidney Lees, also of the Instrumentation Laboratory, would make use of a special application of the root-locus method of servoanalysis to reduce the amount of labor involved in calculating a point by point response of the transient.

Still another method, for which equipment was not available, would again use the analog computer. Here, the transient transfer function would be presented as a function of time by squaring and adding the responses of the two systems, taking the square root of the sum, and applying the resulting signal to one axis of an oscilloscope, the other of which is the time axis.

The remaining material in this chapter is presented not with the idea of showing any quantitative information, but by using the data as obtained to show the manner in which the theory might be applied.

Figure 3-17 is a linear plot of $|F(w, t)|^2$ obtained by the methods of Appendix D. It is from this plot that it is proposed that mean-square errors be determined by the integral of Equation (2-11).

$$M S \text{ output} \Big|_{t=t_1} = \int_0^{\infty} |F(w, t_1)|^2 G_{(in)}(w) dw. \quad (2-11)$$

Figure 3-18 is the more familiar semi-log plot of Fig. 3-17, on which is also plotted, but not to scale, the steady-state transfer function for comparison. Thus, it is seen that the apparent spikes in Fig. 3-17 are just such as would occur if the transfer function squared were itself plotted to a linear scale. The shape of the curve at four hours is due to the fact that the maximum initial excursion has not been reached, and further, the particular system under consideration is one for which the time to reach the initial peak decreases with increasing frequency over the range considered. It is interesting to note that the remaining curves for 12, 24, and 36 hours generally follow the shape of the transfer function.

Figures 3-19 through 3-21 are the plots of the areas under the curves of Fig. 3-17 for the five sub-systems defined by the terms on the right of the simplified form of Equation (A-38), shown below.

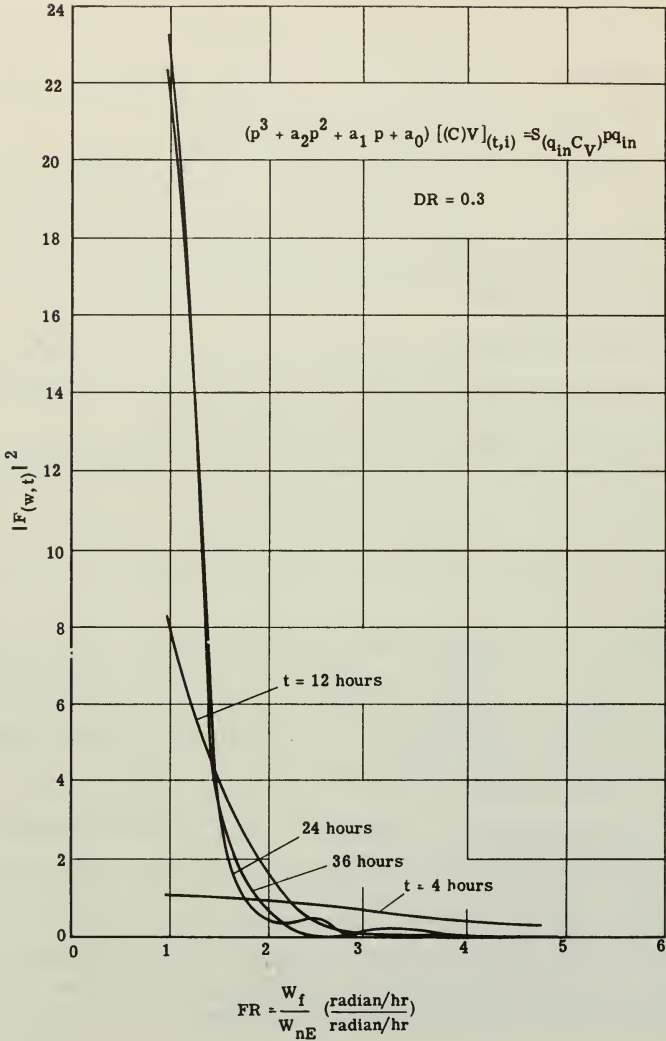


Fig. 3-17 Transient transfer functions squared for $\frac{p}{[P]}$ subsystems of damped vertical indicator, DR = 0.3.

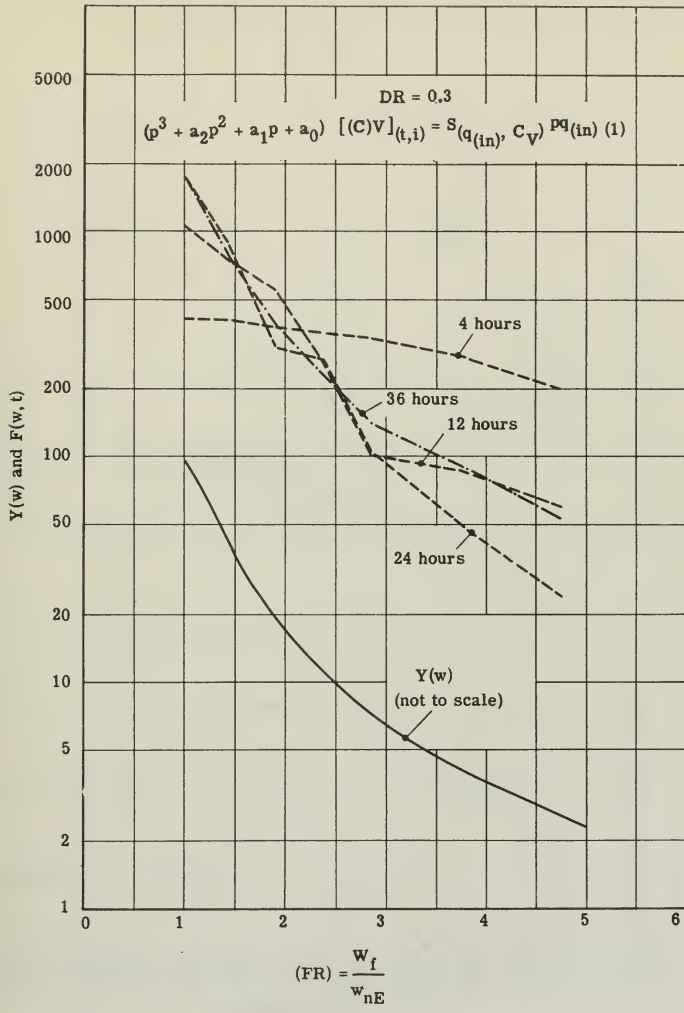


Fig. 3-18 Transient transfer functions for damped vertical indicator, DR = 0.3.

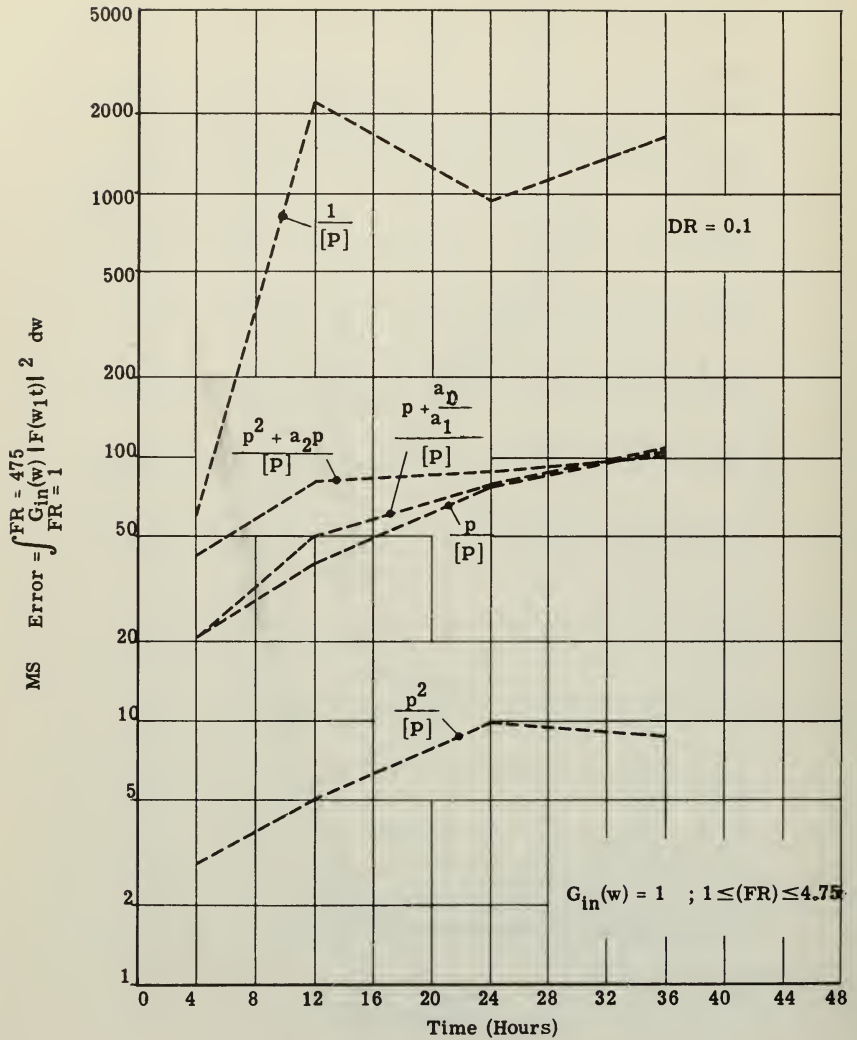


Fig. 3-19 Ensemble mean square errors in damped vertical indicator, DR = 0.1.

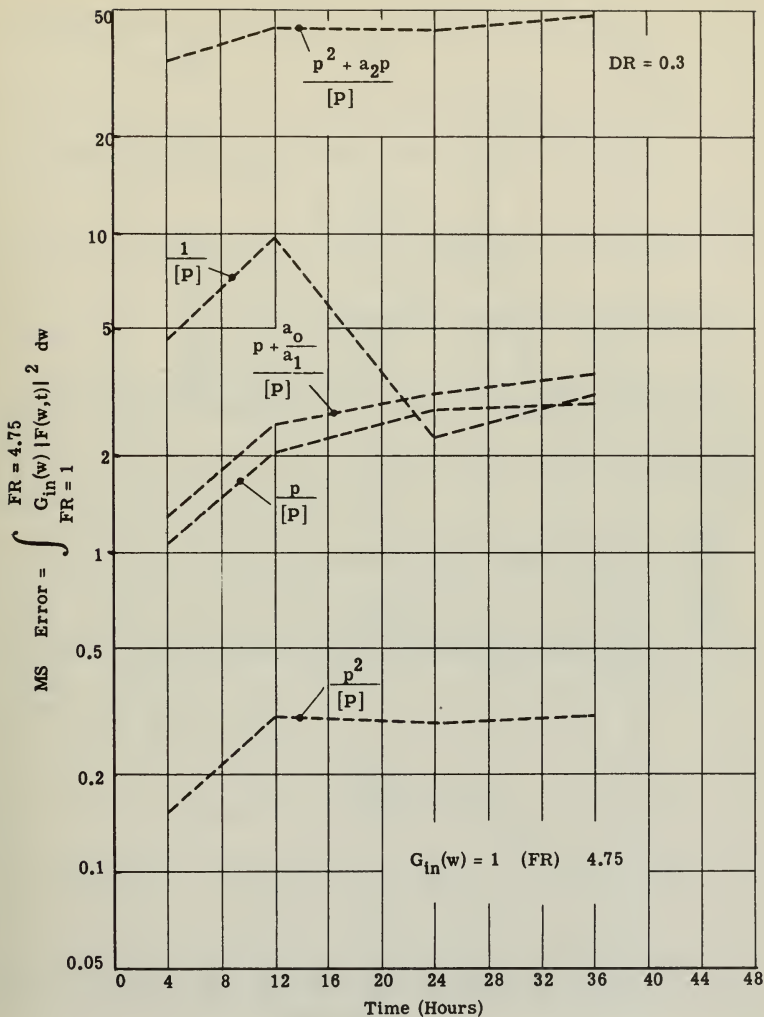


Fig. 3-20 Ensemble mean square errors in damped vertical indicator, DR = 0.3.

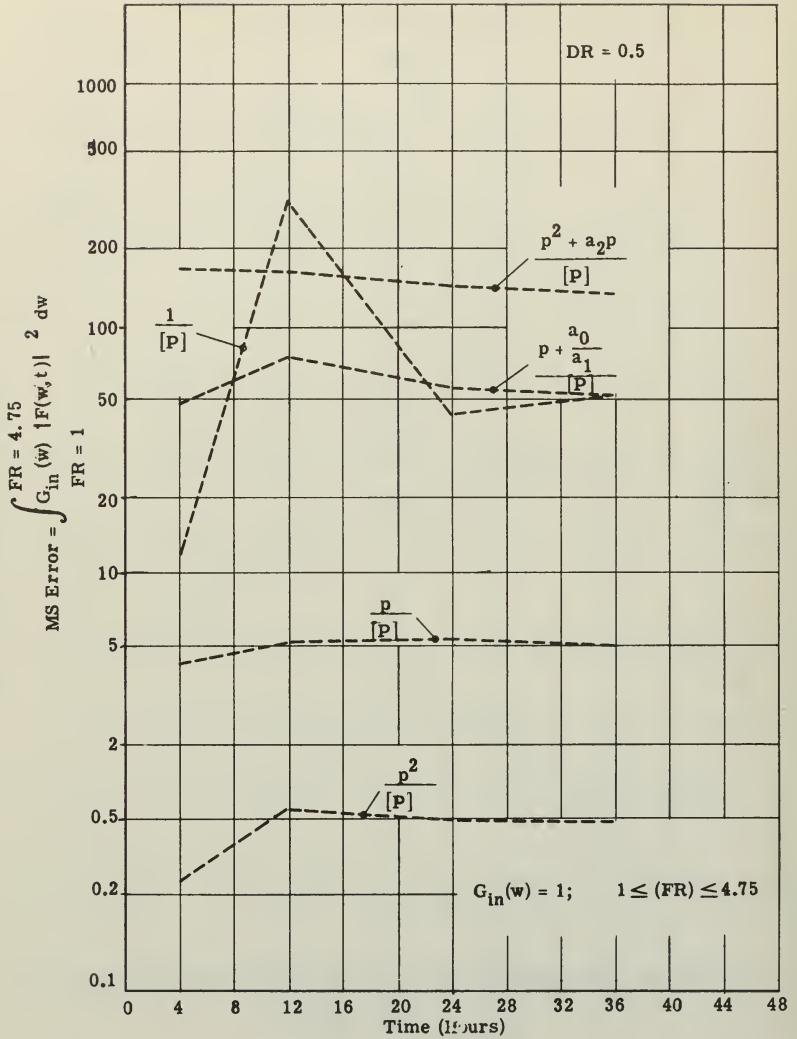


Fig. 3-21 Ensemble mean square errors in damped vertical indicator, DR = 0.5.

$$\begin{aligned}
[(C)V]_{(t, i)} = & S_{(q_{(in)}, C_V)} \frac{1}{[P]} q_{(in)0} + S_{(q_{(in)}, C_V)} \frac{p}{[P]} q_{(in)1} + \\
& + S_{(q_{(in)}, C_V)} \frac{p^2}{[P]} q_{(in)2} + S_{(q_{(in)}, C_V)} \frac{(p + \frac{a_0}{a_1})}{[P]} q_{(in)(1, 0)} + \\
& + S_{(q_{(in)}, C_V)} \frac{(p^2 + a_2p)}{[P]} q_{(in)(2, 1)}, \tag{A-38}
\end{aligned}$$

where $[P] \equiv$ characteristic differential equation for the vertical indicator.

Following the definition of Equation (2-11), the plots of the areas may be assigned the special significance of the mean-square error in vertical indication at each time, $t = 4, 12, 24,$ and 36 hours, for an input with power spectral density such that $G_{(in)}(w) = 1$ for $1 \leq (FR) \leq 4.75$, and is everywhere else equal to zero.

The reader will note the similarity between the shapes of the error curves for corresponding systems at different damping ratios, and further, the apparent trend in the relative location of the curves at each damping ratio. However, considering the accuracy of the data involved, it is doubtful that more than a tentative conclusion can be drawn as to the relative importance of the sub-systems as error sources until further work is done along this line.

APPENDIX A

VERTICAL INDICATION

BASIC PRINCIPLES

The following principles of vertical indication were set forth in Reference(15), and are repeated here for completeness. Figure A-1 is a sketch of a three-axis vertical indicator.

The vector angle representing the correction to the indicated vertical is expressed mathematically as

$$\overline{[(C)V]}_{(t,i)} = \bar{1}_{V_t} \times \bar{1}_{V_i}, \quad (A-1)$$

where the quantities are defined as in Fig. A-2.

Indication with Respect to Earth Axes — Accelerometer Tracking

The rate of change of this angle with respect to indicated position axes, i. e. , in a set of coordinates that consists of the indicated vertical and two other mutually orthogonal axes arbitrarily oriented in the indicated horizontal plane, is

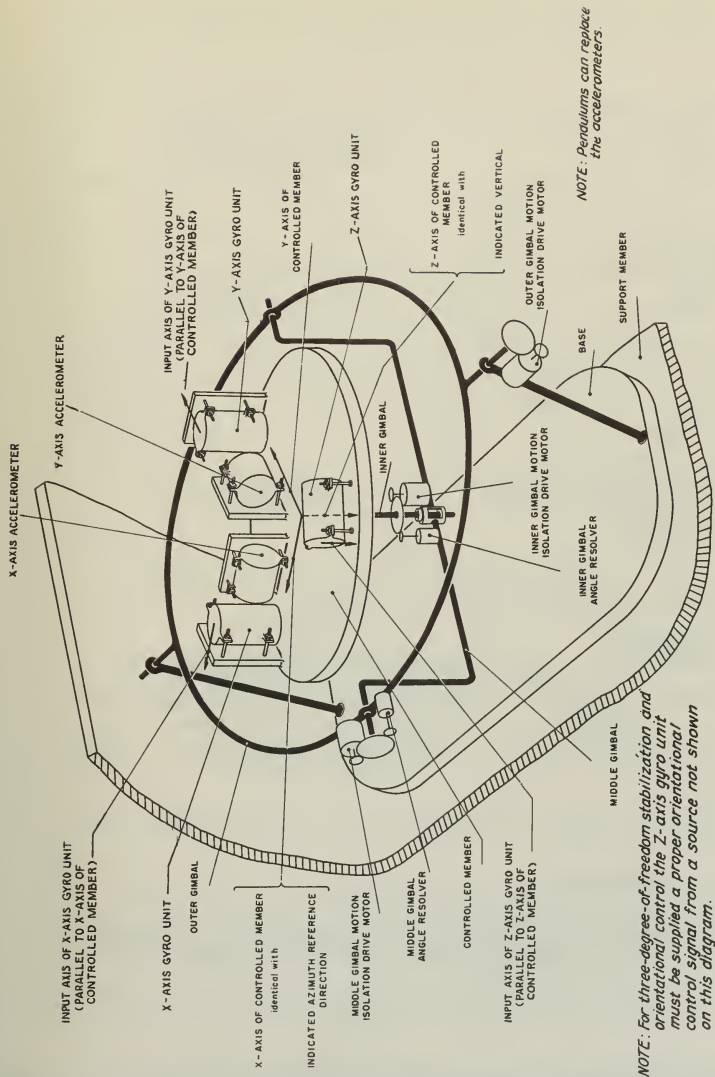
$$\overline{[(C)V]}_{(t,i)P_i} = \bar{W}_{(EV)t} - \bar{W}_{(EV)i} - \bar{W}_{(EP)V_i} \times \overline{[(C)V]}_{(t,i)}, \quad (A-2)$$

where $\overline{[(C)V]}_{(t,i)P_i}$ = rate of change of indicated vertical correction with respect to indicated position axes,

$\bar{W}_{(EV)t}$ = angular velocity of true vertical with respect to the Earth,

$\bar{W}_{(EV)i}$ = angular velocity of indicated vertical with respect to the Earth,

$\bar{W}_{(EP)V_i}$ = angular velocity of indicated position axes with respect to the Earth about the indicated vertical.



NOTE: Pendulums can replace the accelerometers

NOTE: For three-degree-of-freedom stabilization and orientational control the Z-axis gyro unit must be supplied a proper orientational control signal from a source not shown on this diagram.

Fig. A-1 Line schematic diagram showing essential geometrical parts of a complete vertical indicating system using two single-axis accelerometers and three single-degree-of-freedom gyro units.

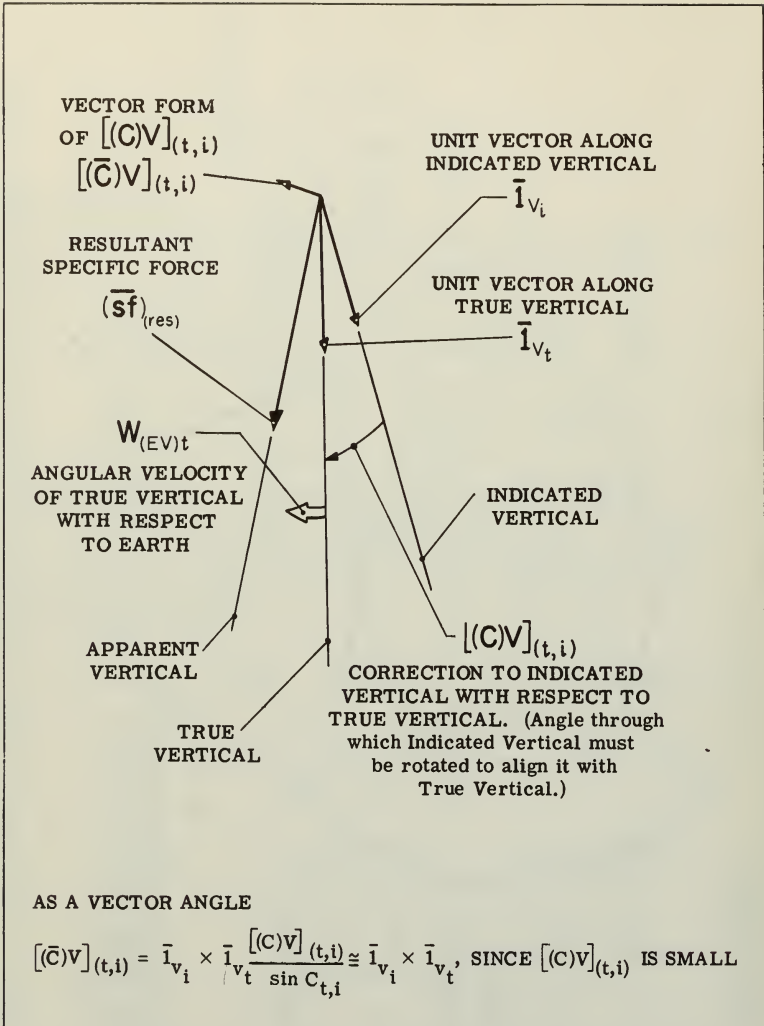


Fig. A-2 Geometrical relationships associated with the vector angle form of the correction to the indicated vertical with respect to the true vertical.

The magnitude of the indicated horizontal component of the resultant specific forces, i. e., the quantity sensed by an accelerometer, is expressed mathematically in Equation (A-3).

$$(\text{sf})_{(\text{res})H_i} = \left| (\overline{\text{sf}})_{(\text{res})H_i} \right| = \left| \bar{1}_{V_i} \times (\overline{\text{sf}})_{(\text{res})} \right|, \quad (\text{A-3})$$

where

$$\begin{aligned} (\text{sf})_{(\text{res})H_i} &= \text{indicated horizontal component of resultant specific force,} \\ \left| \quad \quad \quad \right| &= \text{denotes magnitude of the enclosed vector quantity.} \end{aligned}$$

Let the system operate such that the angular velocity of the indicated vertical with respect to the Earth is a function of the magnitude of the indicated horizontal component of the resultant specific force and directed so as to rotate the indicated vertical toward the resultant specific force vector, namely

$$\bar{W}_{(EV)i} = (\text{PF})_{(Vi)}(f, W) \left| \bar{1}_{V_i} \times (\overline{\text{sf}})_{(\text{res})} \right|, \quad (\text{A-4})$$

where

$$(\text{PF})_{(Vi)}(f, W) = \text{vertical-indicating performance function for a specific force input and an angular velocity output.}$$

Substitution of Equation (A-4) into Equation (A-2), plus the relationships for the resultant specific force from Derivation 1, gives

$$\begin{aligned} \left[\overline{(\dot{C})V} \right]_{(t, i)P_i} &= \bar{W}_{(EV)t} - (\text{PF})_{(Vi)}(f, W) \bar{1}_{V_i} \times \left\{ \bar{g} - (\dot{\bar{W}}_{EP})_E \times \bar{R}_E \right. \\ &\left. - \bar{W}_{EP} \times (\bar{W}_{EP} \times \bar{R}_E) - 2\bar{W}_{IE} \times (\bar{W}_{EP} \times \bar{R}_E) \right\} - \bar{W}_{(EP)V_i} \times \left[\overline{(\dot{C})V} \right]_{(t, i)}. \end{aligned} \quad (\text{A-5})$$

The specific force components in Equation (A-5) can be conveniently resolved into components parallel to the true vertical and perpendicular to the true vertical (the arbitrary nature of axes in the horizontal plane requires no further subdivision into components), namely,

$$\begin{aligned} \bar{g} &= \bar{1}_{V_t} g, \\ \bar{R}_E &= -\bar{1}_{V_t} R_E, \end{aligned}$$

$$\bar{W}_{EP} = \bar{1}_{V_t} W_{(EP)V_t} + \bar{W}_{(EV)t}$$

Substitution of these relationships into Equation (A-5) gives the specific force in terms of components along the true vertical, along the angular velocity vector of the true vertical (which must be perpendicular to the true vertical) and perpendicular to both of these, namely,

$$\begin{aligned} [(\dot{C}\bar{V})]_{(t,i)P_i} = & \bar{W}_{(EV)t} - (PF)_{(Vi)(f,W)} \bar{1}_{V_i} \times \left\{ \bar{1}_{V_t} [g - R_E W^2_{(EV)t} \right. \\ & - 2R_E (\bar{W}_{IE}) \cdot \bar{W}_{(EV)t}] + \bar{W}_{(EV)t} R_E [W_{(EP)V_t} + 2(\bar{W}_{IE} \cdot \bar{1}_{V_t})] \\ & \left. + [(\dot{W}_{EP})_E \times \bar{1}_{V_t}] R_E \right\} - \bar{W}_{(EP)V_i} \times [(\overline{C}\bar{V})]_{(t,i)}. \end{aligned} \quad (A-6)$$

Carrying out the vector operation indicated in Equation (A-6), regrouping terms and omitting the components parallel to the indicated vertical as not being applicable to the indication of the vertical gives

$$\begin{aligned} [(\dot{C}\bar{V})]_{(t,i)P_i} + (PF)_{(Vi)(f,W)} (sf)_{(res)V_t} [(\overline{C}\bar{V})]_{(t,i)} = & \bar{W}_{(EV)t} \\ & - (PF)_{(Vi)(f,W)} R_E (\dot{W}_{(EV)t}) P_i - (PF)_{(Vi)(f,W)} R_E [W_{(EP)V_t} \\ & + 2(\bar{W}_{IE} \cdot \bar{1}_{V_t})] (\bar{1}_{V_i} \times \bar{W}_{(EV)t}) - \bar{W}_{(EP)V_i} \times [(\overline{C}\bar{V})]_{(t,i)}, \end{aligned} \quad (A-7)$$

where

$$(sf)_{(res)V_t} = g - R_E W^2_{(EV)t} - 2R_E (\bar{W}_{IE} \cdot \bar{W}_{(EV)t}), \quad (A-8)$$

= component of resultant specific force along the true vertical.

Let $(PF)_{(Vi)(f,W)}$ be the following operator:

$$(PF)_{(Vi)(f,W)} = S_{(Vi)(f,W)} \int_{P_i} () dt, \quad (A-9)$$

where \int_{P_i} denotes integration of a function of the indicated axes with respect to the time. Substitution of Equation (A-9) into Equation (A-7) gives Equation (A-10):

$$\begin{aligned}
& \overline{[(\dot{C}\dot{V})]}_{(t,i)P_i} + S_{(Vi)(f,\dot{W})} \int_{P_i}^{(sf)_{(res)}V_t} \overline{[(C)V]}_{(t,i)} dt = \overline{W}_{(EV)t} \\
& - S_{(vi)(f,\dot{W})} \int_{P_i} R_E \overline{(\dot{W})}_{(EV)t} P_i dt - S_{(vi)(f,\dot{W})} \int_{P_i} R_E \overline{W}_{(EP)V_t} \\
& + 2(\overline{W}_{IE} \cdot \overline{1}_{V_t}) (\overline{1}_{V_i} \times \overline{W}_{(EV)t}) dt - \overline{W}_{(EP)V_i} \times \overline{[(C)V]}_{(t,i)}. \quad (A-10)
\end{aligned}$$

Differentiating (A-10) with respect to the time gives the differential performance equation in terms of functions of the indicated axes:

$$\begin{aligned}
& \overline{[(\dot{C}\dot{V})]}_{(t,i)P_i} + S_{(Vi)(f,\dot{W})} (sf)_{(res)}V_t \overline{[(C)V]}_{(t,i)} \\
& = (1 - S_{(vi)(f,\dot{W})} R_E) \overline{(\dot{W})}_{(EV)t} P_i - S_{(vi)(f,W)} R_E \overline{W}_{(EP)V_t} \\
& + 2(\overline{W}_{IE} \cdot \overline{1}_{V_t}) (\overline{1}_{V_i} \times \overline{W}_{(EV)t}) - \overline{W}_{(EP)V_i} \times \overline{[(C)V]}_{(t,i)P_i}, \quad (A-11)
\end{aligned}$$

where it is assumed that variations in R_E are slow enough to be treated as quasi-static and variations in $(sf)_{(res)}V_t$ are either slow enough to be quasi-static or fast enough to be ineffective.

For Schuler-tuning let

$$S_{(vi)(f,\dot{W})} = \frac{1}{R_S},$$

where R_S is a set value made as nearly equal as possible to the magnitude of R_E . If it is then assumed that $R_S = R_E$, Equation (A-11) becomes

$$\begin{aligned}
& \overline{[(\dot{C}\dot{V})]}_{(t,i)P_i} + \frac{(sf)_{(res)}V_t}{R_S} \overline{[(C)V]}_{(t,i)} = - \overline{W}_{(EP)V_t} + 2(\overline{W}_{IE} \cdot \overline{1}_{V_t}) (\overline{1}_{V_i} \\
& \times \overline{W}_{(EV)t}) - \overline{W}_{(EP)V_i} \times \overline{[(C)V]}_{(t,i)P_i}. \quad (A-12)
\end{aligned}$$

The terms $\overline{W}_{(EP)V_t} (\overline{1}_{V_i} \times \overline{W}_{(EV)t})$ and $2(\overline{W}_{IE} \cdot \overline{1}_{V_t}) (\overline{1}_{V_i} \times \overline{W}_{(EV)t})$ are small in comparison with $\frac{(sf)_{(res)}V_t}{R_S}$, and can be neglected. This can be shown as follows:

$\overline{W}_{(EP)V_t}$, the magnitude of the rate of change of the meridian about the true vertical with respect to the Earth, is given by

$$W_{(EP)V_t} = \frac{v_B}{R_E} \sin(\text{Co}) \tan(\text{Lat}), \quad (\text{A-13})$$

where

v_B = Velocity of base,

Co = course of base,

Lat = latitude,

$$W_{(EV)t} = \frac{v_B}{R_E}, \quad (\text{A-14})$$

$$\left| W_{(EP)V_t} (\bar{1}_{V_i} \times \bar{W}_{(EV)t}) \right| \cong W_{(EP)V_t} W_{(EV)t}, \quad (\text{A-15})$$

and

$$\left| 2(\bar{W}_{IE} \cdot \bar{1}_{V_t}) (\bar{1}_{V_i} \times \bar{W}_{(EV)t}) \right| \cong 2W_{(EV)t} W_{IE} \sin(\text{Lat}).$$

Assume that the base is traveling due east at 10 knots at 70° latitude:

$$\frac{W_{(EP)V_t} W_{(EV)t}}{(\text{sf})_{(\text{res})V_t} R_S} = \frac{R_S W_{(EP)V_t} W_{(EV)t}}{(\text{sf})_{(\text{res})V_t}} = 0.02 \text{ min. of arc}, \quad (\text{A-16})$$

$$\frac{2W_{IE} \sin(\text{Lat}) W_{(EV)t}}{(\text{sf})_{(\text{res})V_t} R_S} = \frac{2R_S W_{IE} \sin(\text{Lat}) W_{(EV)t}}{(\text{sf})_{(\text{res})V_t}} = 0.25 \text{ min. of arc}. \quad (\text{A-17})$$

Neglecting the above terms, Equation (A-12) reduces to

$$\overline{[(C)V]}_{(t,i)P_i} + \frac{(\text{sf})_{(\text{res})V_t}}{R_S} \overline{[(C)V]}_{(t,i)} = \overbrace{\overline{W_{(EP)V_i} \times [(C)V]}_{(t,i)}}. \quad (\text{A-18})$$

The term $\overline{W_{(EP)V_i} \times [(C)V]}_{(t,i)}$ represents an orientation transfer, not a magnitude effect, and represents a secondary coupling between the x and y systems. Since this will only produce a "spiraling in" effect as the system approaches its null position, it will be ignored in subsequent discussions.

Equation (A-18) now reduces to

$$\frac{\ddot{}}{[(C)V]_{(t,i)} P_i} + \frac{{}^{(sf)}(res)V_t}{R_s} \overline{[(C)V]_{(t,i)}} = 0. \quad (A-19)$$

INSTRUMENTATION OF A SINGLE-AXIS OF THE VERTICAL INDICATOR OF FIGURE A-1(UNDAMPED)

Definitions of Symbols Used in the Following Derivations

a_c	Coriolis acceleration
a_{EB}	Acceleration of base with respect to Earth
a_{IB}	Acceleration of base with respect to inertial space
P_i	Indicated position (latitude or longitude) of vehicle
$(P_i)_o$	Indicated position of vehicle at start of problem
P_t	True position of base
$[(C)P]_{(t,i)}$	Position correction
$[(C)P]_{(t,i)o}$	Position correction at start of problem
$[(C)V]_{(t,i)}$	Correction to the indicated vertical
$[(C)V]_{(t,i)o}$	Correction to indicated vertical at start of problem
$[(C)V]_{(t,r)}$	Correction to reference vertical
$[(C)V]_{(t,r)o}$	Correction to reference vertical at start of problem
$e()$	Output signal voltage of device indicated by subscript
\bar{G}	Gravitational field vector
\bar{g}	Gravity field vector
H	Angular momentum of gyro unit rotor
$i()$	Output current of device indicated by subscript
M_g	Torque on gyro gimbal
$R = R_E$	Radius of the Earth, a function of geographic position
R_s	Set value of Earth radius used for Schuler-tuning
$S() (,)$	Sensitivity of component or component-group indicated by first subscript, with input and output indicated by second subscript

V_i	Indicated vertical
$(V_i)_0$	Indicated vertical at start of problem
V_r	Reference vertical
V_t	True vertical
$(V_t)_0$	True vertical at start of problem
$W_{(EV)i}$	Angular velocity of indicated vertical with respect to the Earth
$W_{(EV)r}$	Angular velocity of reference vertical with respect to the Earth
$W_{(EV)t}$	Angular velocity of true vertical with respect to the Earth
W_{IB}	Angular velocity of base with respect to inertial space
W_{IE}	Angular velocity of Earth with respect to inertial space
$W_{(IV)i}$	Angular velocity of indicated vertical with respect to inertial space
cmds	Controlled member drive system
(U)	Uncertainty in quantity immediately following.
(I)	Inaccuracy in quantity immediately following.
I_w	Water speed compensation current
hfi	High frequency integrator
lfi	Low frequency integrator
V_w	Velocity of craft through the water
V_c	Velocity of water current
$(U)W_{(gu)}$	Uncertainty in gyro drift
dir	Direct channel amplifier
fb	Feedback amplifier
\dot{e}_{c_p}	Earth rate compensation voltage

Figure 1-3 represents the functional diagram of the instrumentation of a single axis of the complete vertical indicator of Fig. A-1. Figures A-3 and A-4 are the mathematical functional diagrams of Fig. 1-3 for the undamped and damped systems, respectively.

The quantity $[(C)V]_{(t, i)}$ is defined by Equation (A-1); that is, $[(C)V]_{(t, i)}$

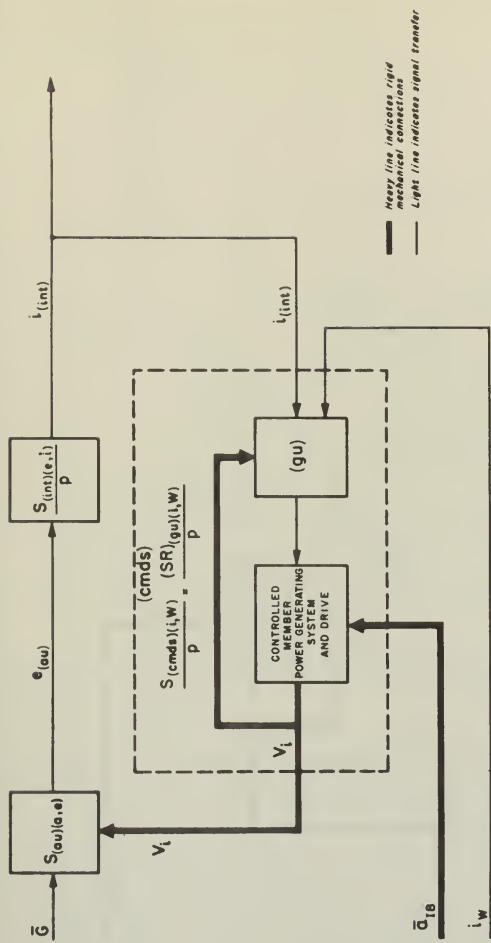


Fig. A-3 Mathematical functional diagram of a basic single-axis undamped vertical indicating system using the components shown in Fig. 1-3.

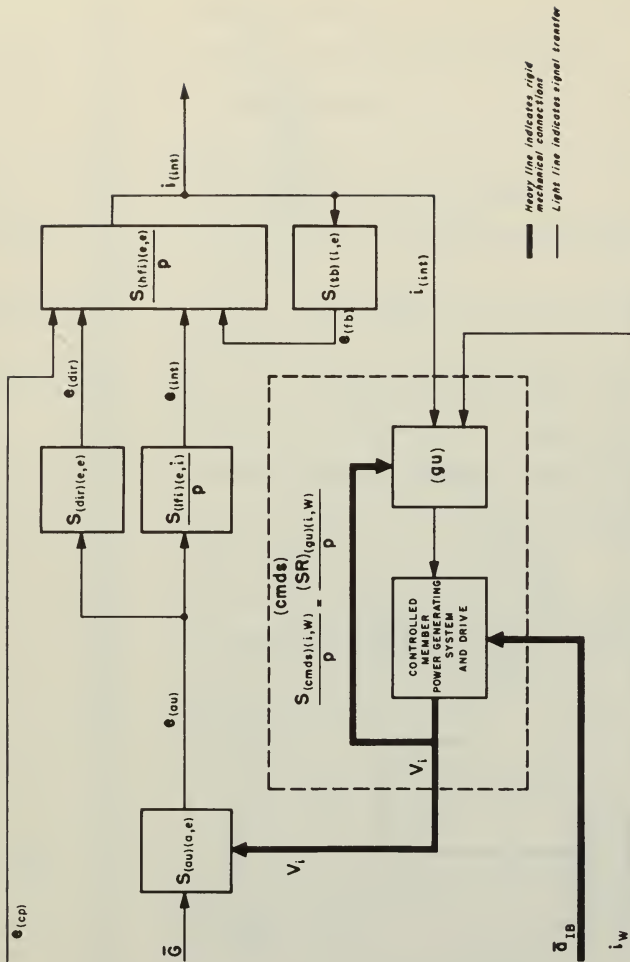


Fig. A-4 Mathematical functional diagram of a basic single-axis damped vertical indicating system using the components shown in Fig. 1-3.

is the angle between the true vertical and the indicated vertical.

Then, in scalar form and operator notation,

$$p[(C)V]_{(t, i)} = W_{(EV)t} - W_{(EV)i}, \quad (A-20)$$

where

$$p = \frac{d}{dt}. \quad (A-21)$$

Equation (A-20) corresponds to Equation (A-2) with the coupling term $(\overline{W}_{(EP)V_i} \times [(C)\overline{V}]_{(t, i)})$ neglected.

The proposed system consists essentially of an accelerometer, an integrator, a single-degree-of-freedom integrating gyro unit, and a drive system for the stable platform or controlled member. The accelerometer is mounted on, and near the axis of rotation of, the controlled member. It will therefore sense the indicated acceleration of the base with respect to inertial space, or the projection of the resultant specific inertia reaction force on the indicated horizontal plane (in general this force will contain both acceleration and gravity effects).

The development of the system equations is shown in Derivation Summary A-I. Equation (A-32) represents the solution of the vertical indicator, which is not presented here as an analytical expression but is rather presented as a series of figures in Chapter 4, and is further discussed there.

INSTRUMENTATION OF A SINGLE-AXIS OF THE VERTICAL INDICATOR OF FIGURE A-1 (DAMPED).

Figure A-4, the mathematical block diagram of a damped single-axis vertical indicator, is essentially a modification of Fig. A-3, the undamped vertical indicator, in which a direct channel and second integration with a feedback loop are added in the orientational control-signal-generating loop to provide damping and stabilization in the system. The essentials of the procedure are as presented in Appendix C.

The development of the equations for instrumentation of this system proceeds in an analogous manner to the development in Part II of this appendix and is presented briefly in Derivation Summary A-II.

Equation (A-38) represents the complete mathematical performance equation of the damped vertical indicator. The solution is not presented here but is discussed further in Chapter 3.

DERIVATION SUMMARY A-I

The performance equation for the accelerometer unit is (neglecting accelerometer dynamics*):

$$e_{(au)} = S_{(au)(a,e)} (g[(C)V]_{(t,i)} + a_{IB})^{**} + (U)e_{(au)}, \quad (A-22)$$

where e_{au} = accelerometer unit output signal,

$S_{(au)(a,e)}$ = accelerometer unit sensitivity for an acceleration input and a voltage output,

a_{IB} = acceleration of the base with respect to inertial space.

Since the system intrinsically minimizes $[(C)V]_{(t,i)}$, this angle will be small enough in general to permit the assumptions:

$$\sin [(C)V]_{(t,i)} \cong [(C)V]_{(t,i)}$$

$$\cos [(C)V]_{(t,i)} \cong 1$$

In Reference 8 it was shown that, at submarine velocities,

$$a_{IB} \cong R p W_{(EV)t} \cdot \quad (A-23)$$

Substituting this in (A-22) gives

$$e_{(au)} = S_{(au)(a,e)} (g[(C)V]_{(t,i)} + R p W_{(EV)t}) + (U)e_{(au)}. \quad (A-24)$$

The integrator performance equation is given by

$$i_{(int)} = S_{(int)(e,i)} \frac{1}{p} (e_{(au)} + (U)e_{(int)(in)}) + i_{(int)}_0, \quad (A-25)$$

* To incorporate Schuler-tuning characteristics, the system is designed to have a natural period of approximately 84 minutes. Therefore, the dynamics associated with the accelerometer unit and the controlled member drive are neglected.

** In this scalar equation the centripetal acceleration due to the Earth's daily rotation is included in g rather than a_{IB} . The net vertical force is effectively g for submarine operation.

where:

$i_{(int)}$ = current output of integrator ,

$S_{(int)(e,i)}$ = sensitivity of integrator for voltage input, current rate output,

$S_{(int)(e,i)}(U)e_{(int)(in)}$ = uncertainty in $i_{(int)}$ due to equivalent voltage input*,

$i_{(int)0}$ = integrator current at start of problem .

The primary purpose of the gyro unit is to provide a means of stabilizing the controlled member against arbitrary motions of the base; however, in the present analysis, the gyro unit is simply considered to be part of the angular velocity generating system. The input current produces a torque on the gyro unit which is balanced by the angular velocity of the controlled member with respect to inertial space, thereby keeping the gyro unit on null.

$$S_{(t_g)(i,M)}[i_{(int)} + i_w] + (U)M_{(g_u)} = HW_{(cmds)} = HW_{(IV)}i \quad (A-26)$$

where

$(U)M_{(g_u)} = H(U)W_{(g_u)}$ = uncertainty torque on gyro gimbal ,

$S_{(t_g)(i,M)}$ = sensitivity of gyro unit torque generator for current input and torque output ,

i_w = current compensating for rotation of earth with respect to inertial space ,

H = angular momentum of gyro unit ,

$W_{(cmds)}$ = angular velocity of controlled member with respect to inertial space ,

$W_{(IV)}i \equiv W_{(cmds)}$ = angular velocity of indicated vertical with respect to inertial space.

Let

$$S_{(cmds)(i,W)} = \frac{S_{(t_g)(i,M)}}{H} \quad (A-27)$$

* c.f. Chapter 2 - Uncertainties in Components

where

$S_{(cmds)(i,W)}$ = sensitivity of controlled member drive system for a current input and an angular velocity output.

From the foregoing,

$$W_{(IV)i} = W_{(EV)i} + W_{IE} = S_{(cmds)(i,W)}(i_{(int)} + i_w) + (U)W_{(gu)}, \quad (A-28)$$

$$i_w = \frac{W_{IE}}{S_{(cmds)(i,W)}} + (I)i_w = \text{compensating current} + \text{inaccuracy in compensating current}, \quad (A-29)$$

$$W_{(EV)i} = S_{(cmds)(i,W)}(i_{(int)} + (I)i_w) + (U)W_{(gu)}. \quad (A-30)$$

Substituting the above relationships into Eq. (A-30), we obtain

$$\begin{aligned} W_{(EV)_t} - p [(C)V]_{(t,i)} &= W_{(EV)_t} - (W_{EV_T} - W_{(EV)_i}) \\ &= S_{(cmds)(i,W)} \frac{S_{(int)(e,i)}}{p} \left[S_{(au)(a,e)} [g[(C)V]_{(t,i)} + R_s p W_{(EV)_t}] \right. \\ &\quad \left. + (U)e_{(au)} + (U)e_{(int)(in)} \right] + S_{(cmds)(i,W)} (I)i_w + (U)W_{(gu)} \\ &\quad + S_{(cmds)(i,W)} i_{(int)o}. \end{aligned} \quad (A-31)$$

Equation (A-31) corresponds to Eq. (A-4). Substituting Eq. (A-31) into Eq. (A-20), differentiating the result and setting

$S_{(au)(a,e)} S_{(int)(e,i)} S_{(cmds)(i,W)} = \frac{1}{R_s}$ for Schuler tuning, we obtain the differential performance equation

$$\begin{aligned} \left[p^2 + \frac{k}{R_s} \right] [(C)V]_{(t,i)} &= \left[1 - \frac{R}{R_s} \right] p W_{(EV)_t} \\ - \frac{1}{R_s S_{(au)(a,e)}} &[(U)e_{(au)} + (U)e_{(int)(in)}] \\ - p [S_{(cmds)(i,W)} (I)i_w + (U)W_{(gu)}] &. \end{aligned} \quad (A-32)$$

Derivation Summary A-II

The performance equation of the accelerometer unit is unchanged by the modifications and is:

$$e_{(au)} = S_{(au)(a,e)} \left[\int (C)V]_{(t,i)} + R_p W_{(EV)}_t \right] + (U)e_{(au)} \quad (A-24)$$

However, the output of the integrator is now:

$$i_{(int)} = \frac{S_{(hfi)(e,i)}}{p} \left(e_{(dir)} + e_{(int)} + e_{(cp)} + (I)e_{(cp)} - e_{(fb)} + (U)e_{(hfi)(in)} \right) + i_{(int)}e \quad (A-33)$$

where

$$e_{(dir)} = S_{(dir)(e,e)} e_{(au)} + (U)e_{(dir)}$$

$$e_{(int)} = \frac{S_{(lfi)(e,e)}}{p} \left(e_{(au)} + (U)e_{(lfi)(in)} \right) + e_{(int)}e$$

$e_{(cp)}$ = signal voltage compensating for ship's speed through the water.

$$e_{(fb)} = S_{(fb)(i,e)} i_{int} + (U)e_{(fb)}$$

$\frac{S_{(nfi)(e,i)}}{p}$ = performance function of high frequency integrator.

$\frac{S_{(lfi)(e,e)}}{p}$ = performance function of low frequency integrator.

The torque balance equation for the gyro unit remains unchanged.

$$(U)M_{(gu)} + S_{(tg)(i,M)} (i_{int} + i_w) = HW_{(cmds)} = HW_{(IV)}i \quad (A-26)$$

Letting $S_{(cmds)(i,W)} = \frac{S_{(tg)(i,M)}}{H}$, we obtain (A-27)

$$W_{(IV)}i = W_{(EV)}i + W_{(IE)} = W_{(Icmds)} \quad (A-28)$$

$$i_w = \frac{W_{IE}}{S_{(cmds)(i,w)}} + (I)i_w, \quad (A-29)$$

$$W_{(EV)i} = S_{(cmds)(i,w)} (i_{(int)} + (I)i_w + (U)W_{(gu)} \quad (A-30)$$

Substituting the above relationships into Eq. (A-30) gives

$$\begin{aligned} & (p + S_{(hfl)(e,i)} S_{(fb)(i,e)}) (W_{(EV)_t} - p [(C)V]_{(t,i)}) \\ &= S_{(hfl)(e,i)} S_{(cmds)(i,w)} (e_{(dir)} + e_{(int)} + e_{(cp)} + (I)e_{(cp)} \\ &\quad - (U)e_{(fb)} + (U)e_{(hfl)(in)}) + ((U)W_{(gu)} + (I)i_w S_{(cmds)(i,w)}) \\ &\quad \times (p + S_{(hfl)(e,i)} S_{(fb)(i,e)}) \\ &= S_{(hfl)(e,i)} S_{(cmds)(i,w)} [(g(C)V]_{(t,i)} + RpW_{(EV)_t}) \\ &\quad \times (S_{(dir)(e,e)} S_{(au)(a,e)} + \frac{S_{(lfi)(e,\dot{e})} S_{(au)(a,e)}}{p}) \\ &\quad + (S_{(dir)(e,e)} + \frac{S_{(lfi)(e,\dot{e})}}{p}) (U)e_{(au)} + \frac{S_{(lfi)(e,\dot{e})}}{p} (U)e_{(lfi)(in)} \\ &\quad + (U)e_{(dir)} + e_{(cp)} + (I)e_{(cp)} - (U)e_{(fb)} + (U)e_{(hfl)(in)} + e_{(int)_o}] \\ &\quad + (p + S_{(hfl)(e,i)} S_{(fb)(i,e)}) (U)W_{(gu)} + S_{(cmds)(i,w)} (I)i_w. \end{aligned} \quad (A-34)$$

$$\text{Setting } S_{(hfl)(e,i)} S_{(cmds)(i,w)} S_{(au)(a,e)} S_{(dir)(e,e)} = \frac{1}{R_s} \text{ for} \quad (A-35)$$

Schuler tuning and differentiating (A-34) and after re-arranging, we get

$$\begin{aligned} & (p^3 + p^2 S_{(hfl)(e,i)} S_{(fb)(i,e)} + p \frac{p}{R_s} + \frac{p}{R_s} \frac{S_{(lfi)(e,\dot{e})}}{S_{(dir)(e,e)}}) [(C)V]_{(t,i)} \\ &= [p^2 (1 - \frac{R}{R_s}) + p (S_{(hfl)(e,i)} S_{(fb)(i,e)} - \frac{R}{R_s} \frac{S_{(lfi)(e,\dot{e})}}{S_{(dir)(e,e)}})] W_{(EV)_t} \end{aligned}$$

$$\begin{aligned}
& - \frac{(U)_e (au)}{R_g S(au)(e,e)} \left(p + \frac{S(lfi)(e,\dot{e})}{S(dir)(e,e)} \right) - p S(hfi)(e,i) S(cmds)(i,w) (U)_e (dir) \\
& + e_{(cp)} + (I)_e (cp) - (U)_e (fb) + (U)_e (hfi)(in) \\
& - S(hfi)(e,i) S(cmds)(i,w) S(lfi)(e,\dot{e}) (U)_e (lfi)(in) \\
& - \left(p^2 + p S(hfi)(e,i) S(fb)(i,e) \right) (U)_w (EV) - S(cmds)(i,w) \\
& \times \left(p^2 + p S(hfi)(e,i) S(fb)(i,e) \right) (I)_i w. \tag{A-36}
\end{aligned}$$

With $R_g = R$ very nearly, Wrigley⁽²⁾ has shown that the term $\left(1 - \frac{R}{R_g}\right)$ will be negligibly small under conditions which will be encountered in service. In Appendix (C), it is shown that it is possible to minimize the term in

$$p \left[S(hfi)(e,i) S(fb)(i,e) - \frac{S(lfi)(e,\dot{e})}{S(dir)(e,e)} \right] W_{(EV)}_t \text{ for any given damping}$$

ratio.

$$\text{But } W_{(EV)}_t = \frac{V_w}{R} + \frac{V_c}{R},$$

where V_w = component of craft velocity with respect to the water perpendicular to input axis of system.,

and V_c = component of current velocity with respect to the earth perpendicular to input axis of system.

$$\text{Now, setting } e_{(cp)} = \left(\frac{S(hfi)(e,i) S(fb)(i,e) - \frac{S(lfi)(e,\dot{e})}{S(dir)(e,e)}}{S(hfi)(e,i) S(cmds)(i,w)} \right) \frac{V_w}{R}. \tag{A-37}$$

the terms in $e_{(cp)}$ and $W_{(EV)}_t$ disappear from Eq. (A-36) leaving only a term

$$p \left(S(hfi)(e,i) S(fb)(i,e) - \frac{S(lfi)(e,\dot{e})}{S(dir)(e,e)} \right) \frac{V_c}{R} \text{ from the term in } W_{(EV)}_t, \text{ which}$$

will in general be negligible, because V_c , the rate of change of current velocity, is in itself generally small, and, in addition, because the coefficient of V_c is optimized (Chapter 4). Note that the effect of any errors in the measurement of (V_w) are considered in the above system equations in the term $(I)_{e(cp)}$.

Equation (A-36) represents the differential performance equation for the system. If now the Laplace transform of the performance equation is taken, the initial conditions appear as follows where now $p \rightarrow$ Laplace operator.

$$\begin{aligned}
 & \left(p^3 + p^2 S_{(hfi)(e,i)} S_{(fb)(i,e)} + p \frac{g}{R_s} + \frac{g S_{(lfi)(e,\dot{e})}}{R_s S_{(dir)(e,e)}} \right) [(C)\dot{V}]_{(t,i)} \\
 & = p \left(S_{(hfi)(e,i)} S_{(fb)(i,e)} - \frac{S_{(lfi)(e,\dot{e})}}{S_{(dir)(e,e)}} \right) \frac{V_c}{R} \\
 & - \left(p + \frac{S_{(lfi)(e,\dot{e})}}{S_{(dir)(e,e)}} \right) \frac{(U)e_{(au)}}{R_s S_{(au)(a,e)}} \\
 & - p S_{(hfi)(e,i)} S_{(cmds)(i,w)} \left[(U)e_{(dir)} + (I)_{e(cp)} - (U)e_{(fb)} \right. \\
 & \left. + (U)e_{(hfi)(in)} \right] - S_{(hfi)(e,i)} S_{(cmds)(i,w)} S_{(lfi)(e,\dot{e})} (U)e_{(lfi)(in)} \\
 & - \left(p^2 + p S_{(hfi)(e,i)} S_{(fb)(i,e)} \right) (U)W_{(gu)} - S_{(cmds)(i,w)} \\
 & \times \left(p^2 + p S_{(hfi)(e,i)} S_{(fb)(i,e)} \right) (I)I_w + [(C)\dot{V}]_{(t,i)o} \\
 & + \left(p + S_{(hfi)(e,i)} S_{(fb)(i,e)} \right) [(C)\dot{V}]_{(t,i)o} + \left(p^2 + p S_{(hfi)(e,i)} S_{(fb)(i,e)} \right. \\
 & \left. + \frac{g}{R_s} \right) [(C)\dot{V}]_{(t,i)o} - \left(S_{(hfi)(e,i)} S_{(fb)(e,i)} - \frac{S_{(lfi)(e,\dot{e})}}{S_{(dir)(e,e)}} \right) \frac{V_{co}}{R} \\
 & + \frac{(U)e_{(au)o}}{R S_{(au)(a,e)}} + S_{(hfi)(e,i)} S_{(cmds)(i,w)} \left((U)e_{(dir)o} + (I)_{e(cp)o} \right)
 \end{aligned}$$

$$\begin{aligned}
& - (U)^e_{(fb)_o} + (U)^e_{(hfi)(in)_o} + (\dot{U})^w_{(gu)_o} \\
& + \left(P + S_{(hfi)(e,i)} S_{(fb)(i,e)} \right) (U)^w_{(gu)_o} + S_{(cmds)(i,w)} (I)^i_{(w)_o} \\
& + S_{(cmds)(i,w)} \left(P + S_{(hfi)(e,i)} S_{(fb)(i,e)} \right) (I)^i_{(w)_o} \quad (A-38)
\end{aligned}$$

APPENDIX B

POSITION INDICATION BY OPEN-CHAIN INTEGRATION OF THE INDICATED VERTICAL

Figures B-1 and B-2 are the mathematical functional diagrams of the proposed position indicators corresponding to the damped and undamped vertical indicators respectively, as described in Appendix A.

Derivation Summary B-I presents the mathematical derivation of position indication as derived for both systems. This derivation has the same form whether the vertical indicator is damped or undamped. This fact is readily apparent when it is recalled that the relationship between the angular velocity of the controlled member and the integrator current is the same regardless of damping. The relationship is given by Equation (A-30).

Equation (B-6) shows that the correction to the indicated position is the sum of the correction to the indicated vertical, initial conditions in position and correction to the vertical, together with the time integral of certain uncertainties and inaccuracies.

Recalling that the transfer function has been defined as the response of the system to the forcing function $e^{j\omega_f t}$, we may write $|F(\omega, t)|$ for the open-chain integrator as $\left| \frac{1}{\omega_f} (1 - e^{j\omega_f t}) \right|$. The mean-square error may then be evaluated quite simply after the method applied to the undamped closed-chain vertical indicator in Chapter 3. That is, the plot of $\left| \frac{1}{\omega_f} (1 - e^{j\omega_f t}) \right|^2$ may be constructed and the integral of Equation (2-11) applied.

$$MS(\text{output}) \Big|_{t=t_1} = \int_0^\infty |F(\omega, t)|^2 G_{(\text{in})}(\omega) d\omega, \quad (2-11)$$

where $G_{(\text{in})}$ represents the power spectral density of each of the uncertainties shown in Equation (B-5) taken in turn.

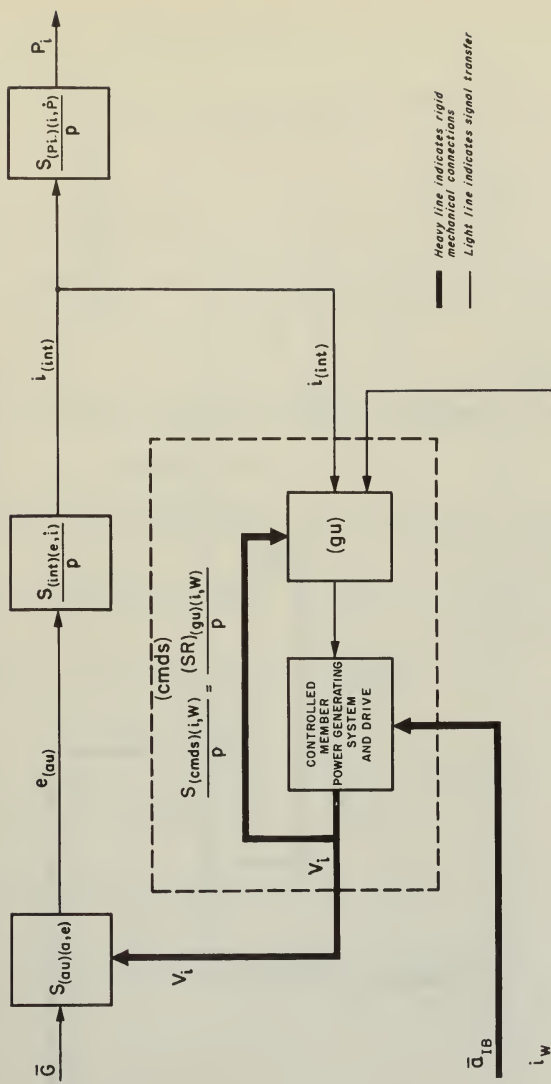


Fig. B-1 Mathematical functional diagram of an undamped system for indicating position by means of an open-chain integration of the angular velocity of the indicated vertical.

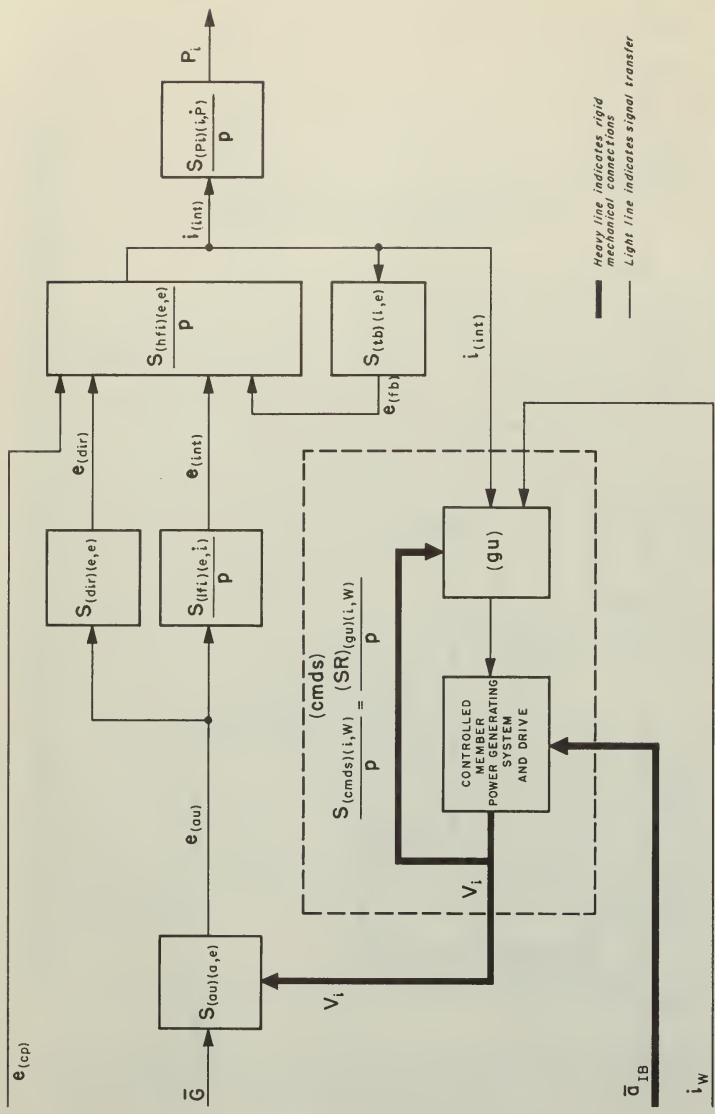


Fig. B-2 Mathematical functional diagram of a damped system for indicating position by means of an open-chain integration of the angular velocity of the indicated vertical.

Derivation Summary B-1

Position Indication by Open-Chain Single Integration
of the Indicated Vertical

In both the systems of Figs. B-1 and B-2, position information is obtained from a single integration of the current input to the gyro unit.

Writing the differential performance equation for the open chain integration:

$$P_i = \frac{S(P_i)(i, \dot{P})}{p} (i_{(int)} + (U)i_{(P_i)(in)}) + (P_i)_o \quad (B-1)$$

where $(U)i_{(P_i)(in)}$ = uncertainty in output of the position indicating integrator reduced to an equivalent signal input,

$(P_i)_o$ = initial position.

From Eq. (A-30), and noting that $w_{(EV)i} = w_{(EV)t} - p[(C)V]_{(t,i)}$ from Eq. (A-20),

$$i_{(int)} = \frac{1}{S_{(cmds)(i,w)}} (w_{(EV)t} - p[(C)V]_{(t,i)} - (U)w_{(gu)}) - (I)i_w \quad (B-2)$$

Substituting Eq. (B-2) into Eq. (B-1) and arbitrarily setting

$S_{(cmds)(i,w)} = S_{(P_i)(i, \dot{P})}$, we obtain

$$P_i = \frac{1}{p} (w_{(EV)t} - p[(C)V]_{(t,i)} - (U)w_{(gu)} + (U)i_{(P_i)(in)} - S_{(P_i)(i, \dot{P})} (I)i_w) + (P_i)_o \quad (B-3)$$

Noting that $\frac{1}{p} w_{(EV)t} = P_t - (P_t)_o$, we write

$$\frac{1}{p} (p[(C)V]_{(t,i)}) = [(C)V]_{(t,i)} - [(C)V]_{(t,i)_o}$$

$$P_i = P_t - (P_t)_o - [(C)V]_{(t,i)} + [(C)V]_{(t,i)_o} + P_{i_o}$$

$$+ \frac{1}{p} \left((U)i_{(P_i)(i_n)} - (U)W_{(g_u)} - S_{(P_i)(i,\dot{P})} (I)i_w \right). \quad (B-4)$$

Further, defining $[(C)P]_{(t,i)} = P_t - P_i$,

$[(C)P]_{(t,i)_o} = (P_t)_o - (P_i)_o$, we can write

$$[(C)P]_{(t,i)} = [(C)P]_{(t,i)_o} + [(C)V]_{(t,i)} - [(C)V]_{(t,i)_o}$$

$$- \frac{1}{p} \left((U)i_{(P_i)(i_n)} - (U)W_{(g_u)} - S_{(P_i)(i,\dot{P})} (I)i_w \right). \quad (B-5)$$

Writing this in the more conventional form we get

$$[(C)P]_{(t,i)} = [(C)P]_{(t,i)_o} + [(C)V]_{(t,i)} - [(C)V]_{(t,i)_o}$$

$$- \int_0^t \left((U)i_{(P_i)(i_n)} - (U)W_{(g_u)} - S_{(P_i)(i,P)} (I)i_w \right) dt. \quad (B-6)$$

APPENDIX C

OPTIMIZATION OF SYSTEM PARAMETERS

In any dynamical system, the engineer is forced to a compromise between a system with minimum forced or steady-state errors and a satisfactory transient response.

Given a performance function of the form

$$[\text{PF}]_{(q_{\text{in}}; q_{\text{out}})} = \frac{C_0 p^n + C_1 p^{n-1} + \dots + C_n}{(1 + S_0) p^n + S_1 p^{n-1} + \dots + S_n} = \frac{q_{\text{(out)}}(p)}{q_{\text{(in)}}(p)}, \quad (\text{C-1})$$

Blasingame⁽¹⁾ has concluded that an optimum practical system may be achieved with a performance function whose characteristic equation is a cubic; and furthermore, such a system may be achieved by a network involving only integrators and summing devices, as shown in Fig. C-1, where the C's and S's may have all values, positive or negative, including zero.

Such an optimum system has been applied to the undamped vertical indicator of Fig. A-3 to obtain the damped vertical indicating system of Fig. A-4.

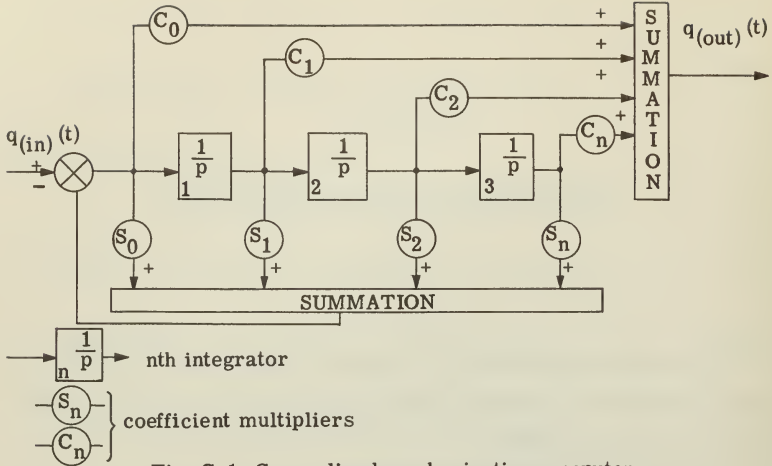


Fig. C-1 Generalized mechanization computer.

The performance equation for the vertical indicator of Fig. A-4 for an input in the angular velocity of the true vertical may be written

$$\frac{[(C)V]_{(t,i)}}{W(EV)_t} = \frac{p^2(1-S_{(vi)(a,W)}^R) + p\left(\frac{1}{\tau_d} - \frac{S_{(vi)(a,W)}^R}{\tau_n}\right)}{p^2 + 2(DR)W_{ns}p + W_{ns}^2} \cdot \frac{1}{p + \frac{1}{(CT)_D}}, \quad (C-2)$$

$$= \frac{p^2(1-S_{(vi)(a,W)}^R) + p\left(\frac{1}{\tau_d} - \frac{S_{(vi)(a,W)}^R}{\tau_n}\right)}{p^3 + \frac{1}{\tau_d}p^2 + \frac{g}{R}p + \frac{1}{\tau_n} \frac{g}{R}}, \quad (C-3)$$

where

$$S_{(vi)(a,W)} = S_{au(a,e)} S_{(dir)(e,e)} S_{(hfi)(e,i)} S_{(cmds)(i,W)},$$

$$\frac{1}{\tau_d} = 2(DR)W_{ns} + \frac{1}{(CT)_D} = \frac{S_{(lfi)(e,\dot{e})}}{S_{(dir)(e,e)}}, \quad (C-4)$$

$$\frac{1}{\tau_n} = \frac{W_{ns}^2}{W_{nE}^2} \frac{1}{(CT)_D} = S_{(hfi)(e,i)} S_{(fb)(i,e)} , \quad (C-5)$$

$$(CT)_D = \frac{2(DR) W_{ns}}{W_{nE}^2 - W_{ns}^2} , \quad (C-6)$$

W_{ns} \equiv natural angular frequency of the system,

W_{nE} \equiv earth's natural angular frequency,

$(CT)_D$ \equiv system characteristic time.

The p^2 term in the numerator of Equation (C-2) has the significance of an acceleration in the angular velocity of the true vertical and gives rise to errors known as jerk-errors in the system. The p term in the numerator of Equation (C-2) has the significance of a rate of change in the angular velocity of the true vertical and gives rise to errors in the system known as velocity errors.

The physical significance of the two changes associated with the angular velocity of the true vertical may be seen if it is recalled that movement of a craft over the surface of the earth produces a change in the direction of the true vertical. This change in direction or angular velocity of the true vertical may be represented as a vector $\overline{W}_{(EV)_t}$ at right angles to the radius vector of the earth and the velocity vector of the craft, and of magnitude $\left| \frac{V_c}{R_E} \right|$, where $\left| \overline{V}_c \right|$ is the velocity of the craft and $\left| \overline{R}_E \right|$ is the radius of the earth.

Thus, a constant linear acceleration of the craft over the earth results in a steady rate of change in the magnitude of the vector $\overline{W}_{(EV)_t}$, and is physically associated with the p term in the numerator of Equation (C-2). However, maneuvering accelerations normally encountered

on shipboard, say in a change of speed from 5 to 15 knots, involve a rapid change of acceleration from zero to a maximum of about 5 knots per minute, with another rapid drop in acceleration as the new speed is approached. These changes in the rate of acceleration are associated with the p^2 term in the numerator of Equation (C-2), and numerically are considerably greater than the maximum accelerations involved. Similarly, a change of course involves a change in the magnitude of the components of $\bar{W}_{(EV)}_t$ along each of the two horizontal axes of the vertical indicator that is stabilized in azimuth. Thus, a course change also gives rise to both jerk and acceleration errors, in which the rate of change of acceleration will again exceed the acceleration for a normal tactical maneuver.

An examination of Equation (C-2) shows that it should be possible to eliminate one of the terms in the numerator by a proper choice of sensitivities, and then to minimize the effects of the remaining term. A study of acceleration and jerk effects likely to be encountered on shipboard indicates that it may be desirable to proceed on the basis of eliminating the jerk-error term and minimizing the acceleration-error term, as has been done in the following sections.

With the jerk-error term eliminated by setting $S_{(Vi)(a,W)} = \frac{1}{R}$, Equation (C-2) may be written

$$\frac{[(C)V]_{(t,i)}}{W_{(EV)}_t} = \frac{p\left[\frac{1}{\tau_d} - \frac{1}{\tau_n}\right]}{p^2 + 2(DR)W_{ns} + W_{ns}^2 \left(p + \frac{1}{(CT)_D}\right)} \quad (C-7)$$

Letting

$$pjW_f = j(FR)W_{nE} \quad ,$$

W_f = angular frequency of forcing function,

$$(FR) \equiv \frac{W_f}{W_{nE}},$$

$$(FR)_n \equiv \frac{W_{nS}}{W_{nE}},$$

and substituting into Equation (C-7), we obtain

$$\frac{[(C)V]_{(t,i)}}{W_{(EV)_t}} = \frac{\frac{j(FR)W_{nE}}{(CT)_D} \left[\frac{4(DR)^2(FR)_n^2 + (1 - (FR)_n^2)^2}{1 - (FR)_n^2} \right]}{W_{nE}^2 \frac{(FR)_n^2}{(CT)_D} \left(-\frac{(FR)_n^2}{(FR)_n^2} + 1 + j \frac{2(DR)(FR)}{(FR)_n} \right) \left(j(FR)W_{nE}(CT)_D + 1 \right)} \quad (C-8)$$

Hydinger and Webster⁽⁸⁾ have shown that the forcing frequencies in $W_{(EV)_t}$ likely to be encountered on shipboard will be essentially of zero frequency or such that $(FR) > 10$.

Optimizing on the basis of $(FR) > 10$, it may be shown that the following approximations hold:

$$a. \quad (FR)W_{nE}(CT)_D \gg 1$$

$$b. \quad \left(1 - \frac{(FR)_n^2}{(FR)_n^2} \right) \gg 2(DR) \frac{(FR)}{(FR)_n}$$

$$c. \quad \frac{(FR)_n^2}{(FR)_n^2} \gg 1$$

By making use of these approximations, Equation (C-8) is reduced to

$$\frac{[(C)V]_{(t,i)}}{W_{(EV)_t}} = \frac{j \left[\frac{4(DR)^2(FR)_n^2 + (1 - (FR)_n^2)^2}{1 - (FR)_n^2} \right] (FR) W_{nE}}{W_{nE}^2 (FR)_n^2 \left(- \frac{(FR)_n^2}{(FR)_n^2} \right) j (FR) W_{nE} (CT)_D} \quad (C-9)$$

$$= \frac{1}{(CT)_D W_{nE}^2 (FR)^2} \left(\frac{4(DR)^2(FR)_n^2 + (1 - (FR)_n^2)^2}{1 - (FR)_n^2} \right). \quad (C-10)$$

Substituting

$$(CT)_D = \frac{2(DR)W_{ns}}{W_{nE}^2 - W_{ns}^2} = \frac{2(DR)(FR)_n}{W_{nE}[1 - (FR)_n^2]}, \quad (C-6)$$

and rearranging, we obtain

$$\frac{[(C)V]_{(t,i)}}{W_{(EV)_t}} = \frac{1}{2(FR)^2 W_{nE}} \left(4(DR)(FR)_n + \frac{1}{(DR)(FR)_n} - \frac{2(FR)_n - (FR)_n^3}{(DR)} \right). \quad (C-11)$$

Assuming a fixed (DR) and taking the partial derivative of Equation (C-11) with respect to $(FR)_n$, we have the necessary condition for a minimum in $\left(\frac{[(C)V]_{(t,i)}}{W_{(EV)_t}} \right)$ to exist at a given damping ratio.

$$\begin{aligned} \frac{\partial}{\partial (FR)_n} \left(\frac{[(C)V]_{(t,i)}}{W_{(EV)_t}} \right) &= 0 \\ &= \frac{1}{2(FR)^2 W_{nE}} \left(\frac{4(FR)_n^2 (DR)^2 - 1 - 2(FR)_n^2 + 3(FR)_n^4}{(FR)_n^2 (DR)} \right). \end{aligned} \quad (C-12)$$

Solving Equation (C-12) for (DR) as a function of $(FR)_n$, we have

$$(DR)^2 = \frac{1 + 2(FR)_n^2 - 3(FR)_n^4}{4(FR)_n^2} \quad (C-13)$$

Figure C-2 is a plot of (DR) vs. $(FR)_n$ from Equation (C-13). With $(FR)_n = 1$, (DR) = 0, and with these conditions in Equation (C-13), we find $\frac{[(C)V]_{(t,i)}}{W_{(EV)_n}} = 0$. The conditions are essentially those of an undamped Schuler-tuned inertial system, which Wrigley⁽¹³⁾ has shown to be insensitive to a sinusoidal forcing function with an 84.4-minute period corresponding to $(FR)_n = 1$.

However, a condition of zero damping and $(FR)_n = 1$ is neither attainable nor desirable in practice for an inertial system operating over an extended period. Hence, choosing (DR) = 0.1, 0.3, and 0.5 for a comparative study, and utilizing the relationships of Equations (C-16) through (C-18) as shown below, we arrive at Table C-1, which is a tabulation of the system parameters for the vertical indicator of Fig. A-4, as obtained when optimum values of $(FR)_n$ are chosen for the various damping ratios. The resulting characteristic equations are also shown below.

The characteristic equation of (C-2), which is in the form of a cubic, can also be expressed as the product of a second-order term and a first-order term as follows:

$$(p^3 + a_2 p^2 + a_1 p + a_0) = (p^2 + Ap + B)(p + D) ; \quad (C-14)$$

also as

$$(p^2 + AP + B)(p + D) = (p^2 + 2(DR)W_{ns}p + W_{ns}^2)(p + \frac{1}{(CT)_D}) \quad (C-15)$$

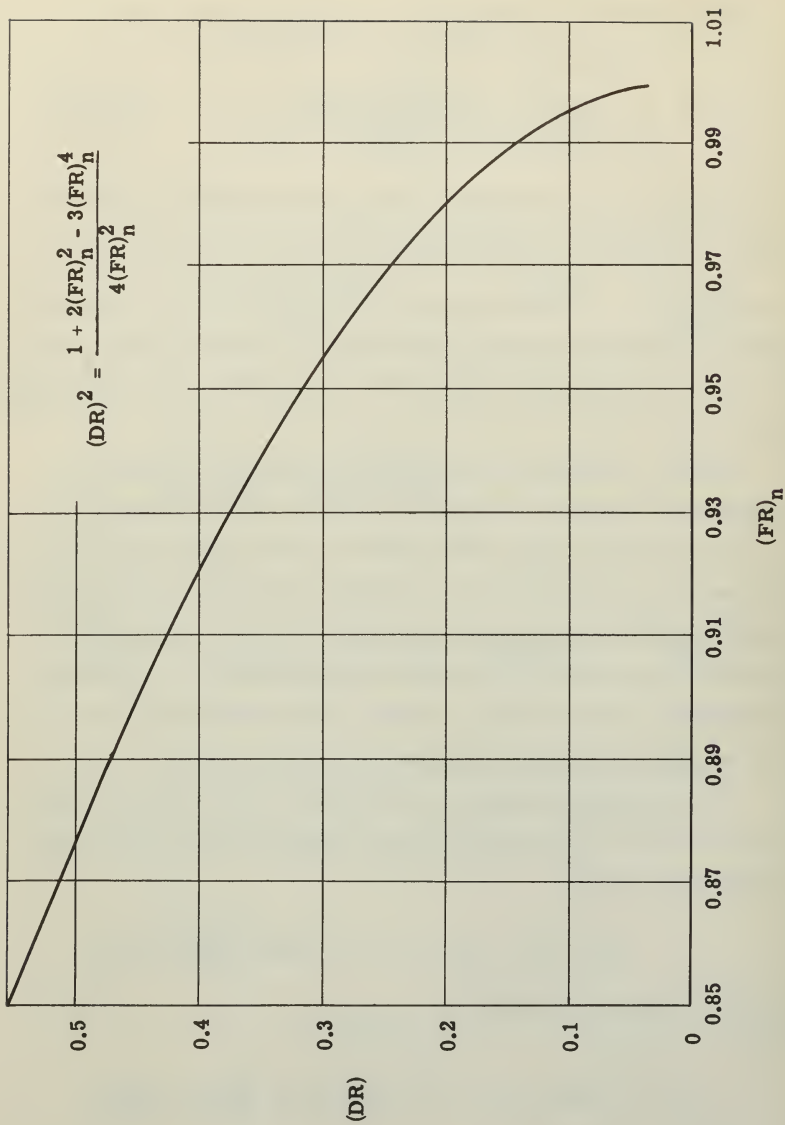


Fig. C-2 Optimum (DR) as a function of $(FR)_n$.

Equating coefficients of like terms, we get

$$a_2 = (A+D) = 2(DR)W_{ns} + \frac{1}{(CT)_D}, \quad (C-16)$$

$$a_1 = (B+AD) = W_{ns}^2 + \frac{2(DR)W_{ns}}{(CT)_D}, \quad (C-17)$$

$$a_0 = (BD) = \frac{W_{ns}^2}{(CT)_D}, \quad (C-18)$$

$$(CT)_D = \frac{2(DR)W_{ns}}{W_{nE}^2 - W_{ns}^2} = \frac{2(DR)(FR)_n}{W_{nE}(1 - (FR)_n^2)}. \quad (C-6)$$

Figures C-3 and C-4 are the resulting steady-state responses of the optimized vertical indicator to sinusoidal forcing motions of the true vertical. It will be noted that the response to accelerations is three orders of magnitude greater than the response to angular velocities at $(FR) = 1$; however, the response to accelerations is decreasing at 18 decibels per octave, whereas the response to velocities is decreasing at 12 decibels per octave. Consequently, at $(FR) = 100$, the responses to both inputs are of equal magnitude, while at higher frequencies the response to accelerations becomes increasingly lower than the response to velocity inputs.

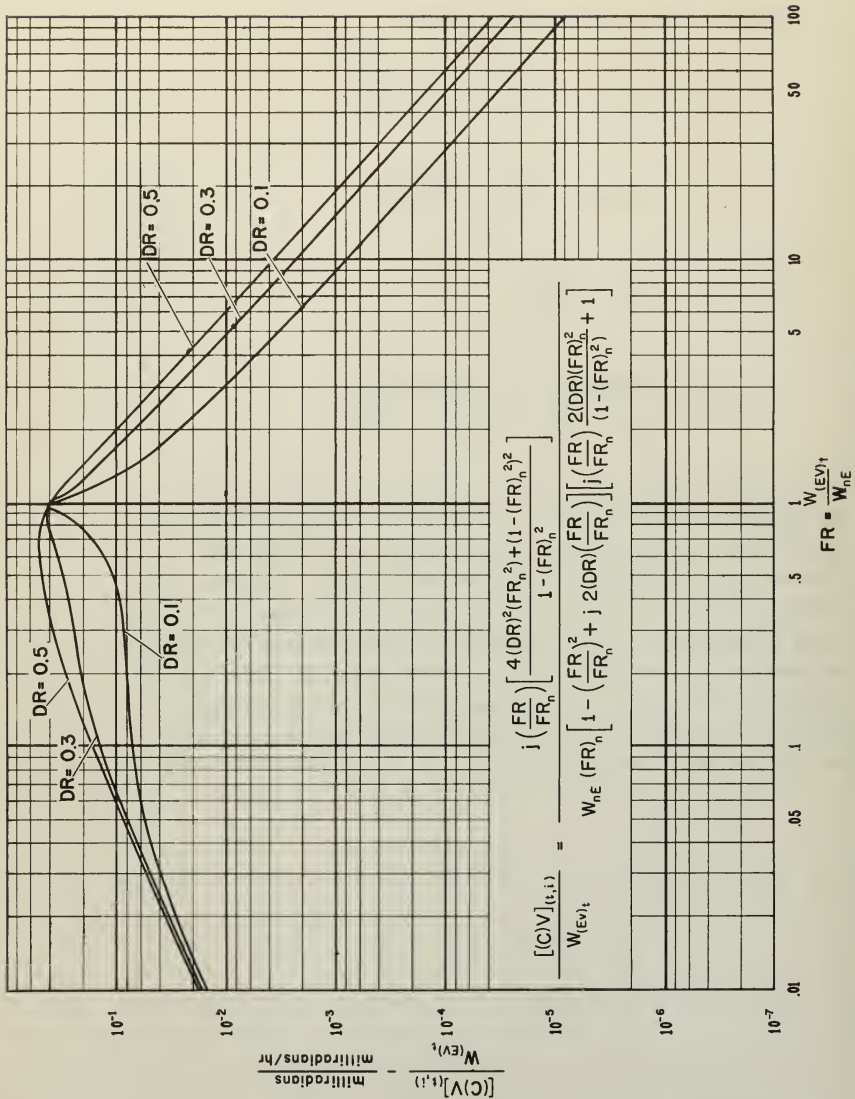


Fig. C-3 Steady-state response of vertical indicator to sinusoidal angular velocity of true vertical.

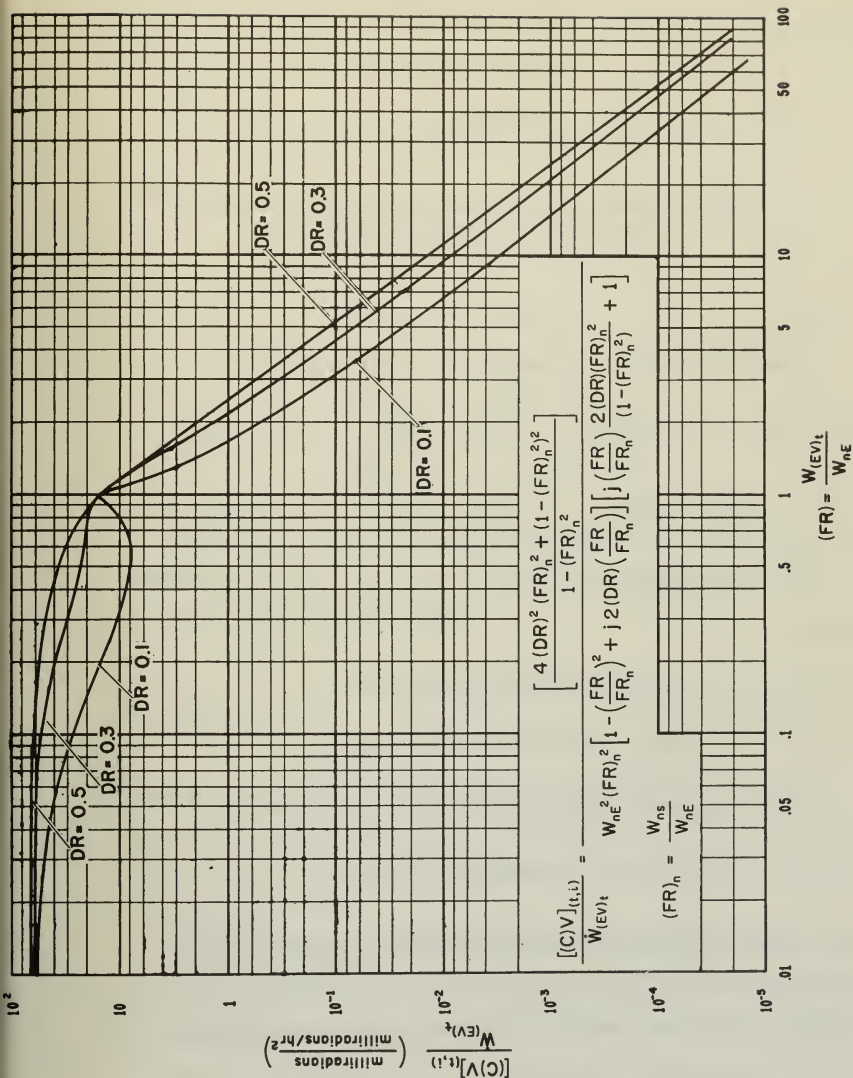


Fig. C-4 Steady-state response of vertical indicator to sinusoidal angular acceleration of true vertical.

APPENDIX D

METHOD USED IN THE DETERMINATION OF SYSTEM PERFORMANCE CHARACTERISTICS

Consider a generalized performance equation of the form

$$\begin{aligned}
 (p^3 + a_2 p^2 + a_1 p + a_0) q(p)_{\text{out}} &= q(p)_{(\text{in}_1)} + p q(p)_{(\text{in}_2)} + (p + a_0) q(p)_{(\text{in}_3)} \\
 &+ p(p + a_1) q(p)_{(\text{in}_4)} - q_{(\text{in}_2)}^{(0+)} - q_{(\text{in}_3)}^{(0+)} - (p + a_1) q_{(\text{in}_4)}^{(0+)} \\
 &- \dot{q}_{(\text{in}_4)}^{(0+)} , \tag{D-1}
 \end{aligned}$$

where

$p \equiv$ Laplace transform variable ,

$q(p)_{\text{in}} \equiv$ Laplace transform of $q(t)_{\text{in}}$,

$q_{(\text{in})}^{(0+)} \equiv$ initial value of $q_{(\text{in})}$ at $t = (0+)$, and

$a_0, a_1, a_2 \dots$ are numerical constants.

The complete response of the differential equation may be found as the sum of the responses to the various terms on the right-hand side of the equation. Thus, the generalized performance equation may be broken down

into a series of performance equations with but a single term on the right, such that $q(p)_{out}$ may be represented as follows:

Setting

$$[P] = (p^3 + a_2p^2 + a_1p + a_0), \text{ the characteristic equation,}$$

we obtain

$$q(p)_{(out_1)} = \frac{1}{[P]}q(p)_{(in_1)}, \quad (D-2)$$

$$q(p)_{(out_2)} = \frac{p}{[P]}q(p)_{(in_2)}, \quad (D-3)$$

$$q(p)_{(out_3)} = \frac{(p + a_0)}{[P]}q(p)_{(in_3)}, \quad (D-4)$$

$$q(p)_{(out_4)} = \text{---- and so forth.}$$

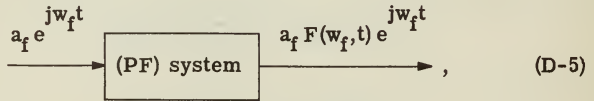
Expressions (D-2), (D-3), and (D-4) show that the generalized system may be considered as made up of a number of independent sub-systems with performance equations given by

$$\frac{1}{p^3 + a_2p^2 + a_1p + a_0}, \quad \frac{p}{p^3 + a_2p^2 + a_1p + a_0}, \quad \text{and} \quad \frac{(p + a_0)}{p^3 + a_2p^2 + a_1p + a_0},$$

respectively. Thus, the weighting function for the generalized system for an input in $q(t)_{(in_n)}$ may be determined quite simply by setting the sub-system of $q(t)_{(in_n)}$ into an analog computer and taking the time response to a unit impulse.

It should be noted here that the terms which have to do with the initial conditions are in the form of a product of a performance equation and a constant, and that the inverse Laplace transform of a constant has the form of an impulse; hence the time response to initial conditions has

the form of a weighting function. Similarly, if $q(t)_{(in)}$ has some probable form that may be predicted on the basis of its physical nature, the probable response of the physical system to $q(t)_{(in)}$ may be found. In particular, if the system inputs and outputs are represented as in the mathematical block diagram of (D-5),



then

$$q(t)_{(out)} = a_f F(w_f, t) e^{jw_f t} = a_f |F(w_f, t)| e^{j(w_f t + A_{dyn})},$$

where

$(PF)_{sys} \equiv$ system performance equation of form of (D-2) etc.,

$F(w_f, t) \equiv$ transient transfer function for frequency w_f (c.f. Chapter 2),

$A_{dyn} \equiv$ dynamic phase angle associated with $F(w_f, t)$;

and, if it is desired to find the absolute value of $F(w_f, t)$ as a function of time for a given frequency w_f , then the output of the system to the forcing function

$$a_f e^{jw_f t} = a_f (\cos w_f t + j \sin w_f t), \quad (D-6)$$

for which the system response may be written

$$q(t)_{(out)} = a_f |F(w_f, t)| \cos(w_f t + A_{dyn}) + j a_f |F(w_f, t)| \sin(w_f t + A_{dyn}), \quad (D-7)$$

may be represented on the complex plane as in Fig. D-1.

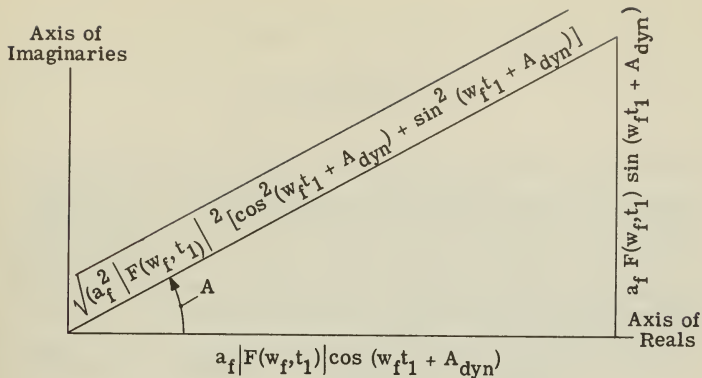


Fig. D-1

Complex plane representation of $F(w_f, t)e^{j w_f t}$.

From Fig. (D-1), it is apparent that

$$\left| q(t)_{\text{out}} \right|_{t=t_1} = \left(a_f |F(w_f, t)| \sqrt{\cos^2(w_f t + A_{\text{dyn}}) + \sin^2(w_f t + A_{\text{dyn}})} \right)_{t=t_1}. \quad (\text{D-8})$$

Solving for $|F(w_f, t)|$, we get

$$\left| F(w_f, t) \right|_{t=t_1} = \left| \frac{q(t)_{\text{out}}}{a_f} \right|_{t=t_1}. \quad (\text{D-9})$$

The mathematical relationships of the foregoing paragraphs suggest that $|F(w_f, t)|$ may be obtained quite simply by use of a high speed analog computer utilizing timing marks to indicate time and clamping to ensure zero initial conditions at the start of each computing cycle.

If the input to the system is chosen as a sinusoidal input of unit amplitude such as $\cos w_f t$, the output will be obtained as a function of time such that

$$q(t)_{\text{out}} = |F(w_f, t)| (\cos w_f t + A_{\text{dyn}}). \quad (\text{D-10})$$

If then the output (D-10) is put through an integrator with the performance function w_f/p , the result will be

$$\begin{aligned}
 q(t)_{\text{out}} &= F(w_f, t) w_f \int_0^t \cos w_f t \, dt \\
 &= |F(w_f, t)| \sin (w_f t + A_{\text{dyn}}). \tag{D-11}
 \end{aligned}$$

If the output (D-10) is now taken to the x-axis input of an oscilloscope and the output (D-11) is taken to the y-axis input of the oscilloscope, the picture on the oscilloscope will be the time varying presentation of Fig. (D-1), where the radius from the center of the diagram to the resulting curve is representative of the sum in Equation (D-7), which has been shown in Equation (D-9) to be equivalent to

$$|F(w_f, t)| = \left| \frac{q(t)_{\text{out}}}{a_f} \right|,$$

or

$$|F(w_f, t)| = |q(t)_{\text{out}}| = \text{radius of oscilloscope curve at}$$

time (t), for a sinusoidal input amplitude.

The function $|F(w, t)|$, which was derived in Chapter 2, may thus be determined by applying unit forcing functions of various frequencies over a frequency band for which the response is desired and taking the amplitude of the radius of the oscilloscope presentation as a function of time.

It is apparent from Fig. D-1 that knowing the frequency and the time for any point on the curve, and having a base line established by some means, the dynamic phase angle may be easily determined from the relationship

$$A_{(\text{dyn})} = A - w_f t.$$

REFERENCE

1. Blasingame, B. P., Optimum Parameters for Automatic Airborne Navigation, Report 6398-T-8, Instrumentation Laboratory, M.I.T., 1950, Secret.
2. Brown, G. S. and Campbell, D. P., Principles of Servomechanisms, John Wiley & Sons, Inc., New York, 1948.
3. Draper, C. S., Notes on Instrument Engineering (Preliminary), Instrumentation Laboratory, M.I.T., September 1950.
4. Dutton, B., Navigation and Nautical Astronomy, U. S. Naval Institute, Annapolis, 1942.
5. Gardner, M. F. and Barnes, J. L., Transients in Linear Systems, Vol. I, John Wiley & Sons, Inc., New York, 1942.
6. Hoag, D. G., Performance Study of Torque Summation Computer, Report 6581-T-1, Instrumentation Laboratory, M.I.T., 1950.
7. Hume, E. L., Illustrative Analysis of a Single Axis Support Motion Isolation System using a Single-Degree-of-Freedom Integrating Gyro Unit as an Angular Deviation Receiver, Report R-7, Instrumentation Laboratory, M.I.T., January 1951, Confidential.
8. Hyding, M. C. and Webster, D. A., High-Accuracy Combined Naval Stable Vertical and East-Seeking Gyrocompass, Report 6671-T-1, Instrumentation Laboratory, M.I.T., 1950. Confidential.
9. James, H. M., Nichols, N. B. and Phillips, R. S., Theory of Servomechanisms, Radiation Laboratory Series, Vol. 25, McGraw-Hill, New York, 1947.
10. Jarosh, J. J., Nugent, J. B., Myers, J. S., Henderson, R. S. and Hoag, D. G., Single-Degree-of-Freedom Integrating Gyro Units for Use in Fire Control Systems, Report R-2, Instrumentation Laboratory, M.I.T., October 1950, Confidential.
11. Lees, S., Integration by the Viscous Shear Process, Report 6398-T-10, Instrumentation Laboratory, M.I.T., 1950.
12. Schuler, M., "Die Störung von Pendel -- und Kreiselapparaten durch

UNCLASSIFIED

die Beschleunigung der Fahrzeuges", Physikalische Zeitschrift, 24, 1923.

13. Wrigley, W., Theoretical Background of Inertial Guidance Systems, Report 6398-S-5, Instrumentation Laboratory, M.I.T., 1950, Confidential.
14. Worthing, A. G., and Geffner, J., Treatment of Experimental Data, John Wiley and Sons, Inc., New York, 1947.
15. Theoretical Background of Inertial Navigation for Submarines, Report R-9, Instrumentation Laboratory, M.I.T., March 1951, Confidential.
16. Anderson, J., Anderegg, J., Whitman, H., Wales, L., Single-Degree-of-Freedom Pendulous Accelerometer Units for use in Aircraft Instrumentation, Stabilization and Control, Report 17 (to be published), Instrumentation Laboratory, M.I.T.

JUL 15 1963
MR 15 63
MR 15 63
1963
27 FEB 73
92 83 1 21

BINDERY
1 2 8 7 3
1 2 8 7 3
6 2 0
23661
23661

Thesis
C7475 Cook 44985
Applications of inertial navigation to underwater warfare.

~~15 1963~~
MR 15 63
1963
27 FEB 73
92 83 1 21

BINDERY
1 2 8 7 3
6 2 0
23661
23661

Thesis
C7475 Cook 44985
Applications of inertial navigation to underwater warfare.

thesC7475

Applications of inertial navigation to u



3 2768 002 09375 9

DUDLEY KNOX LIBRARY